

BBN And The CMB Constrain Neutrino Coupled Light WIMPs

Kenneth M. Nollett^{1,2,3,*} and Gary Steigman^{4,5,†}

¹*Department of Physics and Astronomy, University of South Carolina, 712 Main St., Columbia, SC 29208, USA*

²*Department of Physics and Astronomy, Ohio University, Athens, OH 45701, USA*

³*Department of Physics, San Diego State University, 5500 Campanile Drive, San Diego, CA 92182-1233*

⁴*Center for Cosmology and AstroParticle Physics, Ohio State University,*

⁵*Department of Physics, Ohio State University, 191 W. Woodruff Ave., Columbus, OH 43210, USA*

(Dated: February 13, 2015)

In the presence of a light weakly interacting massive particle, a WIMP with mass $m_\chi \lesssim 30$ MeV, there are degeneracies among the nature of the WIMP (fermion or boson), its couplings to the standard model particles (to electrons, positrons, and photons, or only to neutrinos), its mass m_χ , and the number of equivalent (additional) neutrinos, ΔN_ν . These degeneracies cannot be broken by the cosmic microwave background (CMB) constraint on the effective number of neutrinos, N_{eff} . However, since big bang nucleosynthesis (BBN) is also affected by the presence of a light WIMP and equivalent neutrinos, complementary BBN and CMB constraints can help to break some of these degeneracies. In a previous paper [1] the combined BBN and Planck [2] CMB constraints were used to explore the allowed ranges for m_χ , ΔN_ν , and N_{eff} in the case where the light WIMPs annihilate electromagnetically (EM) to photons and/or e^\pm pairs. In this paper the BBN predictions for the primordial abundances of deuterium and ^4He (along with ^3He and ^7Li) in the presence of a light WIMP that only couples (annihilates) to neutrinos (either standard model – SM – only or both SM and equivalent) are calculated. Recent observational estimates of the relic abundances of D and ^4He are used to limit the light WIMP mass, the number of equivalent neutrinos, the effective number of neutrinos, and the present Universe baryon density ($\Omega_B h^2$). Allowing for a neutrino coupled light WIMP and ΔN_ν equivalent neutrinos, the combined BBN and CMB data provide lower limits to the WIMP mass that depend very little on the nature of the WIMP (Majorana or Dirac fermion, real or complex scalar boson), with a best fit $m_\chi \gtrsim 35$ MeV, equivalent to no light WIMP at all. The analysis here excludes all neutrino coupled WIMPs with masses below a few MeV, with specific limits varying from 4 to 9 MeV depending on the nature of the WIMP. In the absence of a light WIMP (either EM or neutrino coupled), BBN alone prefers $\Delta N_\nu = 0.50 \pm 0.23$, favoring neither the absence of equivalent neutrinos ($\Delta N_\nu = 0$), nor the presence of a fully thermalized sterile neutrino ($\Delta N_\nu = 1$). This result is consistent with the CMB constraint, $N_{\text{eff}} = 3.30 \pm 0.27$ [2], constraining “new physics” between BBN and recombination. Combining the BBN and CMB constraints gives $\Delta N_\nu = 0.35 \pm 0.16$ and $N_{\text{eff}} = 3.40 \pm 0.16$. As a result, while BBN and the CMB combined require $\Delta N_\nu \geq 0$ at $\sim 98\%$ confidence, they disfavor $\Delta N_\nu \geq 1$ at $> 99\%$ confidence. Adding the possibility of a neutrino-coupled light WIMP extends the allowed range slightly downward for ΔN_ν and slightly upward for N_{eff} simultaneously, while leaving the best-fit values unchanged.

arXiv:1411.6005v2 [astro-ph.CO] 12 Feb 2015

* nollett@mailbox.sc.edu

† steigman.1@osu.edu

I. INTRODUCTION

While weakly interacting massive particles (WIMPs, χ) present in some extensions of the standard model (SM) of particle physics are usually very massive, with m_χ in excess of tens or hundreds of GeV, there has been a long and continuing interest in light ($m_e \lesssim m_\chi \lesssim$ tens of MeV) or even very light ($m_\chi \lesssim m_e$) WIMPs [3–14]. More recently, the cosmic microwave background (CMB) has been used to measure the expansion rate of the universe during the acoustic oscillation era, expressed as an effective number of neutrino species, N_{eff} . Such measurements have led to exploration of the effect on N_{eff} of a hypothetical WIMP that is sufficiently light to annihilate after neutrino decoupling and heat either the photons or the SM neutrinos beyond the usual heating from e^\pm annihilation [15–18]. For the standard models of particle physics and cosmology (*i.e.*, no light WIMPs, no equivalent neutrinos), N_{eff} measured in the late Universe is $N_{\text{eff}} = 3$ ¹. In those extensions of the SM containing “dark radiation” whose contribution to the early Universe energy density amounts to that of ΔN_ν “equivalent neutrinos,” it is generally the case that $N_{\text{eff}} > 3$. In Ref. [15] this canonical result was revisited, demonstrating that in the presence of a light WIMP that annihilates only to SM neutrinos, a measurement of $N_{\text{eff}} > 3$ from the CMB temperature anisotropy spectrum can be consistent with $\Delta N_\nu = 0$ (“dark radiation without dark radiation”). It was also shown that in the presence of a sufficiently light WIMP that couples strongly to photons and/or e^\pm pairs, a CMB measurement of $N_{\text{eff}} = 3$ is not inconsistent with the presence of dark radiation ($\Delta N_\nu > 0$) [15]. In other words, the presence of one or more equivalent neutrinos, including “sterile neutrinos”², can be consistent with $N_{\text{eff}} = 3$. Depending on its couplings, the late time annihilation of a light WIMP will heat either the relic photons or the relic neutrinos, and this will affect the CMB constraint on the sum of the neutrino (SM and equivalent) masses [15]. It was emphasized in Ref. [15] that in the presence of a light WIMP and/or equivalent neutrinos there are degeneracies among the light WIMP mass and its nature (fermion or boson, as well as its couplings to e^\pm pairs and photons, or to neutrinos), the number and nature (fermion or boson) of the equivalent neutrinos, and the temperature at which they decouple from the SM particles. Constraints from the CMB alone are insufficient to break these degeneracies.

However, as already shown by Kolb *et al.* [3] and Serpico and Raffelt [4], and more recently by Boehm *et al.* [21], the presence of a light WIMP modifies the early Universe energy and entropy densities (more specifically, the relation between the photon and neutrino temperatures), affecting the synthesis of the light nuclides during big bang nucleosynthesis (BBN). As a result, BBN provides additional constraints on the properties of light WIMPs and equivalent neutrinos that, in combination with the information from later epochs provided by the CMB, can help to break some of these degeneracies. None of the previous studies of BBN in the presence of a light WIMP allowed for equivalent neutrinos, thereby eliminating some potentially interesting possibilities (*e.g.*, sterile neutrinos). In our previous paper [1] we explored the consequences for BBN of equivalent neutrinos, allowing for a light WIMP (a Majorana or Dirac fermion, or a real or complex scalar boson) that remains in thermal equilibrium with e^\pm pairs and photons until a low enough temperature that all the WIMPs have annihilated away (similar to the millicharged, light particle proposed by Dolgov *et al.* [22]). In this paper we turn our attention to light WIMPs that remain in equilibrium with, and annihilate into, either the SM neutrinos or both the SM and equivalent neutrinos (like the “neutrino secret interaction” mediators discussed in Refs. [23, 24]). As in Ref. [1], BBN is revisited, now allowing for neutrino coupled, light WIMPs and equivalent neutrinos. The 68.3% and 95.5% confidence level regions in the multidimensional parameter spaces of various combinations of the WIMP mass (m_χ), the number of equivalent neutrinos (ΔN_ν), the effective number of neutrinos at recombination (N_{eff}), and the baryon density parameter ($\Omega_B h^2$), are identified and compared with the independent constraints on N_{eff} and $\Omega_B h^2$ from the Planck CMB results [2]. In this manner the consistency between the physics and the evolution of the Universe at BBN (\sim first few minutes) and at recombination (\sim 400 thousand years later) is tested, and the allowed ranges and best fit values of the parameters are identified.

In § II, two of the three key parameters explored here, the effective number of neutrinos (N_{eff}) and the number of equivalent neutrinos (ΔN_ν) are defined more precisely, and the influence of a light WIMP on the $N_{\text{eff}} - \Delta N_\nu$ relation is explored. § II A focuses on the effects on the key parameters of a light WIMP that annihilates only to neutrinos (with and without restriction to SM neutrinos³). Since the publication of our previous paper exploring the BBN and CMB constraints on an electromagnetically coupled light WIMP [1], there has been a new determination of the primordial abundance of deuterium [25] that has a small, but non-negligible, effect on the parameter constraints presented there⁴. In § III this new D abundance is used along with the same primordial helium abundance adopted previously [27], to update the BBN constraints on the baryon density and ΔN_ν . These slightly revised BBN constraints are combined with those on the baryon density and N_{eff} from Planck [2] to update the best joint fit values of N_{eff} , ΔN_ν , and

¹ If the assumption of instantaneous neutrino decoupling (IND) at high temperature is relaxed, $N_{\text{eff}} = 3.046$ [19, 29, 30].

² Here, the term sterile neutrinos is reserved for equivalent neutrinos with $\Delta N_\nu = 1$. For several sterile neutrinos, ΔN_ν is an integer, ≥ 1 .

³ A light WIMP that annihilates only to particles in a “dark sector,” not to SM particles (similar to that considered, *e.g.*, in Ref. [33]), is beyond the scope of this paper.

⁴ A subsequent update to the helium abundance, published late in the preparation of this paper, is discussed briefly in § VI.

$\Omega_B h^2$. Then, in §IV, the effects on primordial nucleosynthesis of a neutrino coupled light WIMP are outlined as a function of the WIMP mass for a light WIMP that could be a Majorana or Dirac fermion, as well as a real or complex scalar boson. In §V the joint BBN and CMB constraints on the key parameters are presented. In particular, the *lower* bounds to the masses of the different kinds of neutrino coupled light WIMPs are presented in Table I and the assumptions leading to these bounds are summarized in §V A. Finally, in §VI the results presented here, as well as those updated for an electromagnetically coupled light WIMP, are summarized.

II. REVIEW AND OVERVIEW

In preparation for the results to be presented here, it is important to establish various definitions relevant to the CMB constraints, following the notation of Ref. [15]. The key parameters are the effective number of neutrinos, N_{eff} , and the number of equivalent neutrinos, ΔN_ν . At late times in the early Universe, long after the e^\pm pairs and any light WIMPs have annihilated, the only particles contributing to the radiation energy density are the photons (γ), the three SM neutrinos (ν_e, ν_μ, ν_τ), and ΔN_ν equivalent neutrinos (ξ). At these late times, when $T_\gamma \rightarrow T_{\gamma 0} \ll \{m_e, m_\chi\}$, and $T_{\gamma 0}$ is still greater than the neutrino masses, the radiation energy density, normalized to the energy density in photons alone, is

$$\left(\frac{\rho_R}{\rho_\gamma}\right)_0 = 1 + \left(\frac{\rho_\nu}{\rho_\gamma}\right)_0 \left[3 + \left(\frac{\rho_\xi}{\rho_\nu}\right)_0\right] = 1 + \left(\frac{\rho_\nu}{\rho_\gamma}\right)_0 [3 + \Delta N_\nu]. \quad (1)$$

The “number of equivalent neutrinos” appearing here, ΔN_ν , is defined by the late time (but when the neutrinos are still relativistic) ratio of the energy density in one, or more, extremely relativistic (ER) ξ particles (fermions or bosons) to that in one of the SM neutrinos, $\Delta N_\nu \equiv (\rho_\xi/\rho_\nu)_0$. In the absence of a light WIMP the SM neutrinos decouple at a temperature $T_{\nu d}$, between 2 and 3 MeV, prior to the bulk of the e^\pm annihilation [28]. When the e^\pm pairs annihilate, they (mainly) heat the photons relative to the neutrinos. As a result, although $T_\nu = T_\gamma$ for $T_\gamma \geq T_{\nu d}$, once $T_\gamma < T_{\nu d}$, it is the case that $T_\gamma > T_\nu$. The canonical, textbook assumption is that the SM neutrinos decouple instantaneously, when the only other thermally populated relativistic particles are the photons and the e^\pm pairs, and also that at neutrino decoupling the e^\pm pairs are extremely relativistic ($m_e/T_\gamma \rightarrow 0$). Under these assumptions the neutrino phase space distribution remains that of a relativistic Fermi gas, so that $(\rho_\nu/\rho_\gamma)_0 = 7/8 (T_\nu/T_\gamma)_0^4$, and entropy conservation can be applied to find that, $(T_\nu/T_\gamma)_0^3 = 4/11$. The above result, where e^\pm annihilation heats the photons relative to the decoupled SM and equivalent neutrinos, is used to define the “effective number of neutrinos,” N_{eff} :

$$\left(\frac{\rho_R}{\rho_\gamma}\right)_0 = 1 + \frac{7}{8} \left(\frac{T_\nu}{T_\gamma}\right)_0^4 [3 + \Delta N_\nu] \equiv 1 + \frac{7}{8} \left(\frac{4}{11}\right)^{4/3} N_{\text{eff}}, \quad (2)$$

where,

$$N_{\text{eff}} = \left[\frac{11}{4} \left(\frac{T_\nu}{T_\gamma}\right)_0^3\right]^{4/3} [3 + \Delta N_\nu] = 3 \left[\frac{11}{4} \left(\frac{T_\nu}{T_\gamma}\right)_0^3\right]^{4/3} \left[1 + \frac{\Delta N_\nu}{3}\right] = N_{\text{eff}}^0 \left[1 + \frac{\Delta N_\nu}{3}\right], \quad (3)$$

and (denoting the $\Delta N_\nu = 0$ case with a superscript zero),

$$N_{\text{eff}}^0 = 3 \left[\frac{11}{4} \left(\frac{T_\nu}{T_\gamma}\right)_0^3\right]^{4/3}. \quad (4)$$

It is important to keep in mind that N_{eff} is defined to be a “late-time” quantity, characterizing the SM and equivalent neutrino contributions to the relativistic energy density after BBN has ended, and the e^\pm pairs and any light WIMPs (considered later) have annihilated. The evolution of the energy density during BBN is **not** described as an evolution of N_{eff} with time.

Retaining the assumption of instantaneous neutrino decoupling (IND), but relaxing the assumption that the e^\pm pairs are ER at neutrino decoupling,

$$\left(\frac{T_\nu}{T_\gamma}\right)_0^3 = \frac{4}{2g_s(T_{\nu d}) - 10.5}, \quad (5)$$

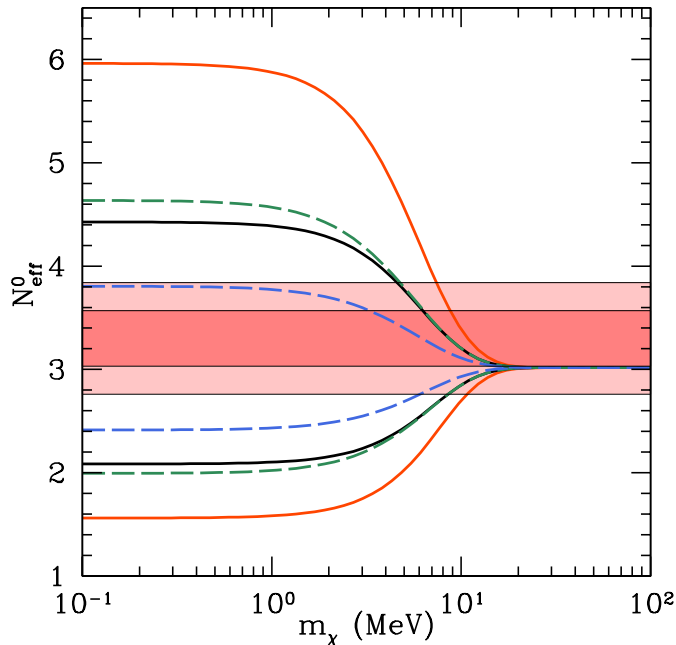


FIG. 1. (Color online) N_{eff}^0 , the value of N_{eff} for $\Delta N_\nu = 0$, as a function of the WIMP mass for WIMPs that annihilate to e^\pm pairs and photons (lower set of curves) and those that annihilate to the SM neutrinos (upper set of curves). For the top set of curves (neutrino coupled), from top to bottom, the solid (red) curve is for a Dirac WIMP, the dashed (green) curve is for a complex scalar, the solid (black) curve is for a Majorana WIMP, and the dashed (blue) curve is for a real scalar. The order of the curves is reversed for the lower set (EM coupled). The horizontal (red/pink) bands are the Planck CMB 68.3% and 95.5% ranges for N_{eff} .

where $g_s(T)$ is defined by the ratio of the total entropy to the entropy in photons alone [1, 15]. In the approximation that $m_e/T_{\nu d} = 0$, $g_s(T_{\nu d}) = 10.75$, so that the canonical results, $(T_\nu/T_\gamma)_0^3 = 4/11$ and $N_{\text{eff}} = 3$, are recovered. However, at $T_{\nu d} \approx 2$ MeV, the electron/positron entropy is already slightly less than the relativistic limit, so that $2g_s(T_{\nu d}) - 10.5 \approx 10.95$, corresponding to $N_{\text{eff}} \approx 3.02$. This is to be compared to the value, $N_{\text{eff}} \approx 3.05$, found [19] when the IND is relaxed and the neutrino phase space density computed in detail, ignoring any equivalent neutrinos. As far as we are aware, no detailed calculation of the neutrino phase space distribution [19, 29, 30] has been published that allows for either equivalent neutrinos or light WIMPs, and such a calculation is beyond the scope of the present work. It is assumed here that $\Delta N_\nu \neq 0$ will not change the literature solutions very much, so $N_{\text{eff}} \approx 3.05(1 + \Delta N_\nu/3)$ is adopted when there is no light WIMP (*i.e.*, for $m_\chi \gtrsim 30$ MeV). However, the IND is used (*e.g.*, in Eq. (3)) whenever there is a light WIMP. In the IND approximation with decoupling at $T_{\nu d} = 2$ MeV, the high WIMP mass limit is $N_{\text{eff}} \approx 3.02(1 + \Delta N_\nu/3)$. The difference between these approximations ($\approx 0.03 + 0.01 \Delta N_\nu$) is very small compared with the errors in the present BBN and CMB constraints on N_{eff} , but may need to be accounted for when higher precision data become available.

In the presence of a light Majorana WIMP that annihilates to e^\pm pairs and/or photons (*i.e.*, is EM coupled), the photons are further heated relative to the already decoupled SM and equivalent neutrinos, and N_{eff}^0 is a function of the WIMP mass (see, *e.g.*, [1, 15] for details). In this case

$$N_{\text{eff}}^0 = 3 \left[\frac{11}{4} \left(\frac{T_\nu}{T_\gamma} \right)_0^3 \right]^{4/3} = 3 \left[\frac{11}{10.95 + 3.5 \phi_{\chi d}} \right]^{4/3}, \quad (6)$$

where $\phi_{\chi d}$ is the ratio of the entropy carried by the light WIMP at $T_{\nu d}$ to the entropy it would have contributed were it massless. The $N_{\text{eff}}^0 - m_\chi$ relation is shown for several possibilities of EM coupled WIMPs by the lower set of curves in Figure 1. In the high mass limit, $N_{\text{eff}}^0 \rightarrow 3.02$. In the limit of very low WIMP mass, $N_{\text{eff}}^0 < 3.02$, ranging from $N_{\text{eff}}^0 \approx 1.6$ to $N_{\text{eff}}^0 \approx 2.4$, with the value depending on the statistics obeyed by the WIMP.

An “equivalent neutrino”, ξ , is a very light ($m_\xi \ll m_e$) particle that is still ER when $T = T_{\gamma 0}$ (*i.e.*, at BBN and at recombination, but not necessarily at present) and is not included in the SM. Such particles could be populated

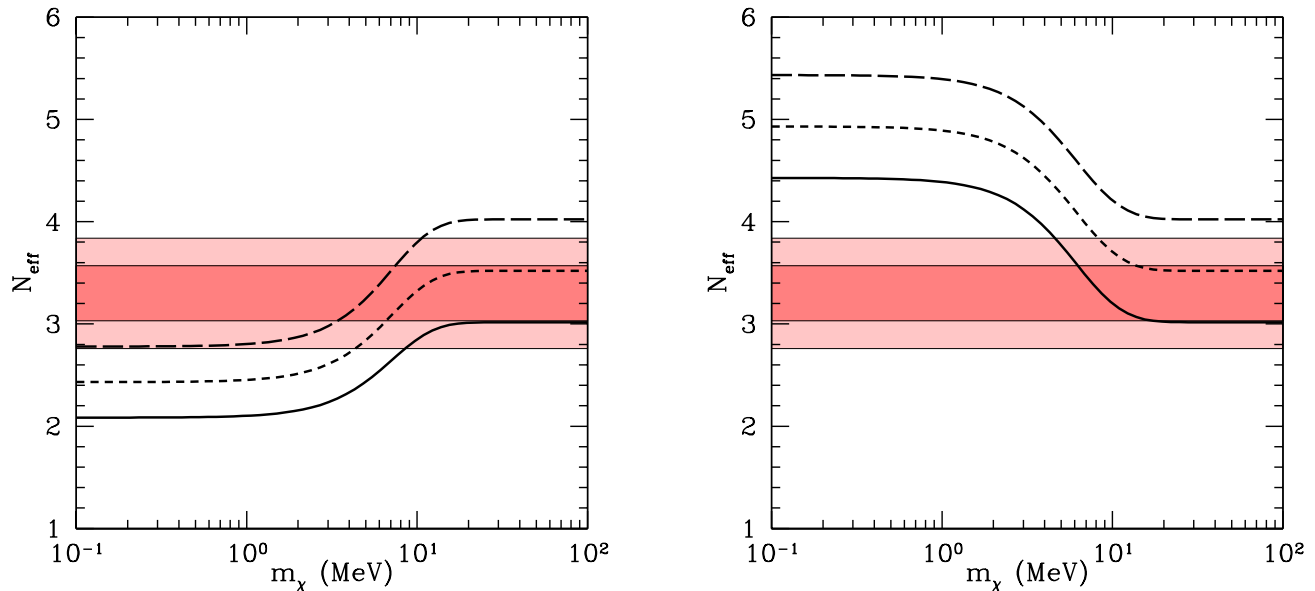


FIG. 2. (Color online) The left panel shows N_{eff} as a function of the WIMP mass for an electromagnetically coupled, Majorana fermion WIMP and ΔN_ν equivalent neutrinos. The solid curve is for $\Delta N_\nu = 0$, the short-dashed curve is for $\Delta N_\nu = 1/2$, and the long-dashed curve is for $\Delta N_\nu = 1$. The horizontal, red/pink bands are the Planck CMB 68.3% and 95.5% allowed ranges for N_{eff} . The right panel shows the corresponding results for a neutrino coupled, Majorana fermion WIMP.

by mixing with the SM neutrinos (*e.g.*, [20]). In this case, each Majorana equivalent neutrino contributes $\Delta N_\nu \leq 1$. Alternatively, they may have once been in equilibrium with the SM particles at a high temperature, but decoupled before the SM neutrinos decoupled, at a temperature $T_{\xi d} \geq T_{\nu d}$. In either case, it is assumed that the equivalent neutrinos are already decoupled from all SM particles when the SM neutrinos decouple. For WIMPs that annihilate exclusively to e^\pm pairs and photons, neither the SM nor equivalent neutrinos are heated after $T_{\nu d}$, and Eq. (6) for N_{eff}^0 becomes a function $N_{\text{eff}}^0(m_\chi)$, differing from $N_{\text{eff}}^0 = 3.02$. The $N_{\text{eff}} - m_\chi$ relation is shown for three values of ΔN_ν in the left hand panel of Fig. 2. For this case, BBN and the CMB were used in our previous paper [1] to constrain N_{eff} and ΔN_ν , where it was found that since $N_{\text{eff}}^0 < 3$ in the presence of an EM coupled light WIMP, at low m_χ , $\Delta N_\nu > 0$ is allowed, and even required, in order to match the measured N_{eff} .

A. Neutrino Coupled Light WIMPs

If, instead, the SM neutrinos are heated by the annihilation of neutrino coupled WIMPs, the case explored here, there are two possibilities. If the WIMP annihilation heats SM neutrinos, but not the already decoupled equivalent neutrinos, then the $N_{\text{eff}} - \Delta N_\nu$ relation [15] is modified, to

$$N_{\text{eff}} = 3.02 \left[\left(1 + \frac{4\tilde{g}_\chi \phi_{\chi d}}{21} \right)^{4/3} + \frac{\Delta N_\nu}{3} \right], \quad (7)$$

where $\tilde{g}_\chi = 1, (7/4, 2, 7/2)$ if the WIMP is a real scalar (Majorana fermion, complex scalar, Dirac fermion). Note that this equation has a different form than Eq. 3. N_{eff} for $\Delta N_\nu = 0$ (*i.e.*, N_{eff}^0) is shown as a function of the WIMP mass for neutrino coupled WIMPs by the upper set of curves in Fig. 1. N_{eff} is shown as a function of the WIMP mass for a Majorana WIMP, for nonzero values of ΔN_ν , in the right hand panel of Fig. 2.⁵

⁵ The version of this graph that appeared in our previous paper [1] contained an error in the calculation of the $\Delta N_\nu \neq 0$ curves. This error affected nothing else in that paper.

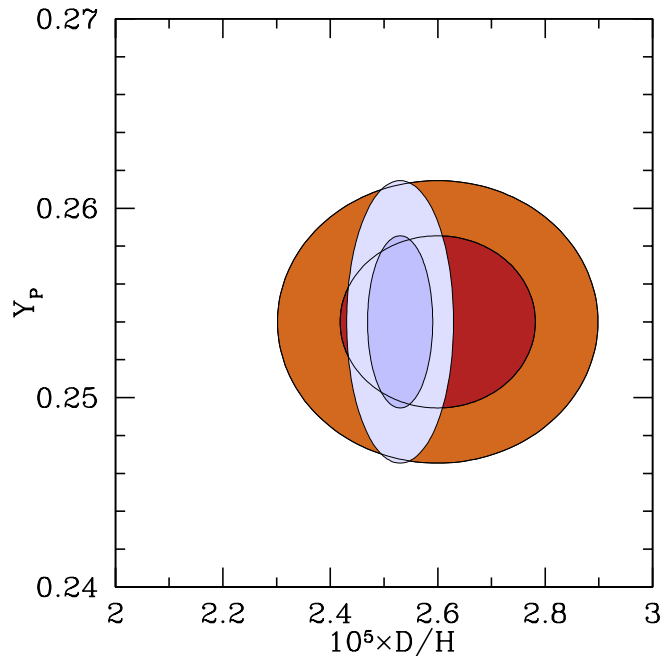


FIG. 3. (Color online) The 68.3% and 95.5% likelihood contours of the observationally inferred primordial abundances of ${}^4\text{He}$ and D in the $Y_{\text{P}} - \text{D}/\text{H}$ plane. The helium abundance, $Y_{\text{P}} = 0.254 \pm 0.003$, is adopted from Izotov *et al.* [27]. The red/orange contours are for the older, Pettini & Cooke [47] D abundance, $y_{\text{DP}} \equiv 10^5 (\text{D}/\text{H})_{\text{P}} = 2.60 \pm 0.12$, and the blue contours correspond to the newer, Cooke *et al.* [25] determination, $y_{\text{DP}} = 2.53 \pm 0.04$.

The other possibility is that the annihilating WIMP heats both the SM and the equivalent neutrinos. In this case

$$N_{\text{eff}} = 3.02 \left(1 + \frac{\Delta N_{\nu}}{3} \right) \left[1 + \frac{4\tilde{g}_{\chi}\phi_{\chi d}}{21 + 7\Delta N_{\nu}} \right]^{4/3}. \quad (8)$$

Note that when $\Delta N_{\nu} = 0$, both results reduce to $N_{\text{eff}}^0 = 3.02(1 + 4\tilde{g}_{\chi}\phi_{\chi d}/21)^{4/3}$. The difference between these two possibilities when $0 \leq \Delta N_{\nu} \leq 1$ is so small that it is invisible on the scale of Fig. 2. This reflects the physics involved: the entropy carried initially by the WIMPs is shared among more species in the second case, but each species receives less entropy. As far as the expansion rate of the universe is concerned, these two effects very nearly cancel. It will be seen below that since the two scenarios for WIMP coupling to neutrinos are equivalent if either $m_{\chi} \rightarrow \infty$ (no light WIMP) or $\Delta N_{\nu} = 0$ (no equivalent neutrinos), there is almost no difference between them in fitting the present data. A curiosity of assuming equilibrium between the WIMPs and all neutrinos (SM plus equivalent) is that it implies a common temperature for all neutrino species and therefore restriction of ΔN_{ν} to integers or integer multiples of $4/7$; in computing this scenario, we have kept ΔN_{ν} as a continuous parameter by allowing arbitrary real values for the spin degeneracy factor of the equivalent neutrinos.

As may be seen from Fig. 2, while $\Delta N_{\nu} \gtrsim 1$ is allowed by the CMB for an EM coupled light WIMP, values of $\Delta N_{\nu} \gtrsim 1$ are disfavored in the presence of a neutrino coupled light WIMP. Indeed, even for $\Delta N_{\nu} = 0$, a neutrino coupled WIMP cannot be very light before coming into conflict with the CMB constraint on N_{eff} . This will become clearer when the BBN and CMB results are compared and combined.

III. UPDATED CONSTRAINTS WITH AND WITHOUT AN EM COUPLED LIGHT WIMP

In our previous paper [1] the consequences for BBN and the CMB, with and without a light WIMP that annihilates to e^{\pm} pairs and/or directly to photons, was explored. Recently, there has been a new determination of the primordial deuterium abundance [25], whose central value is in excellent agreement with the value adopted in [1], but whose uncertainty has been reduced by a factor of three. Confidence level contours of the observationally determined primordial abundances of D and ${}^4\text{He}$ are shown in Figure 3, comparing the older, Pettini & Cooke D abundance

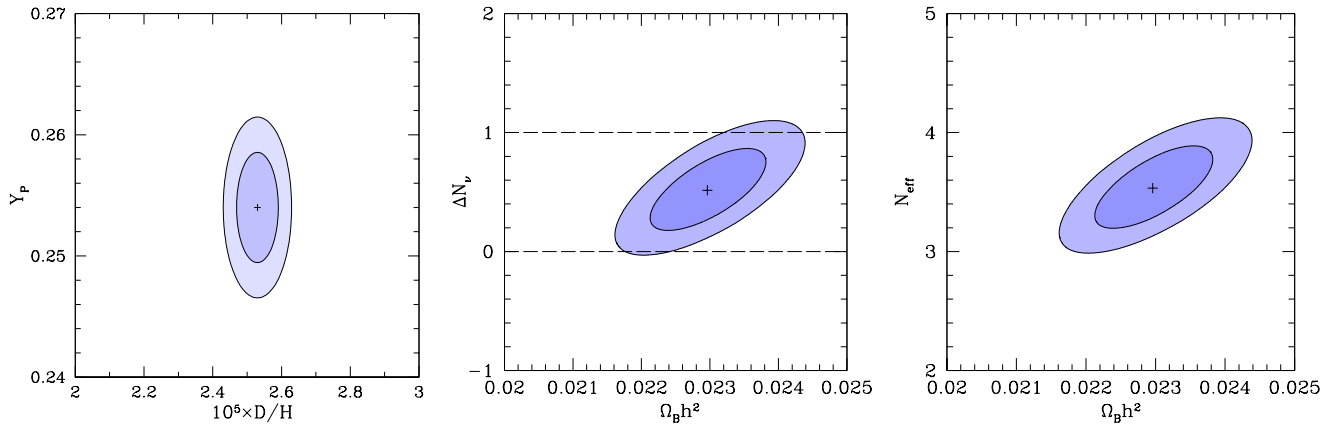


FIG. 4. (Color online) The left hand panel shows the 68.3% and 95.5% likelihood contours in the helium abundance – deuterium abundance ($Y_P - y_{DP}$) plane. The black cross corresponds to $Y_P = 0.254$ [27] and $10^5(D/H)_P = 2.53$ [25]. See the text for details. The middle panel shows the corresponding BBN-inferred 68.3% and 95.5% contours for ΔN_ν and $\Omega_B h^2$, in the absence of a light WIMP and in the IND approximation. The dashed horizontal lines show $\Delta N_\nu = 0$ and $\Delta N_\nu = 1$ as guides to the eye. The right hand panel shows the corresponding contours for N_{eff} and $\Omega_B h^2$. The black crosses in the middle and right hand panels show the best fit BBN values; without the IND approximation, they would fall at $\Delta N_\nu = 0.50$, $N_{\text{eff}} = 3.56$, and $\Omega_B h^2 = 0.0229$.

[47], to the newer, Cooke *et al.* value [25]. This small difference in the D abundance and the large reduction in its uncertainty lead to a small, but noticeable, effect on the central values, and a larger effect on the errors, in the observationally inferred model parameters. In addition to the influence of the equivalent neutrino and WIMP energy densities, the BBN yields depend on the baryon density of the universe, expressible as the ratio, by number, of baryons to photons, $\eta \equiv 10^{10} \eta_{10}$. This ratio and the baryon mass density parameter $\Omega_B h^2$ are related by $\eta_{10} \approx 273.9 \Omega_B h^2$ [26]. To a good approximation, adopting the new D abundance determination in a BBN-only fit increases η_{10} by ~ 0.1 ($\Omega_B h^2$ increases by ~ 0.0004) and results in a decrease in ΔN_ν (and N_{eff}) of order ~ 0.01 [25]. In § III A and § III C the BBN and the joint BBN and CMB constraints are updated.

A. Updated BBN And CMB Constraints In The Absence Of A WIMP

First, assume that there is no light WIMP. Recall that for this case, $N_{\text{eff}} = 3.05(1 + \Delta N_\nu/3)$. In the left hand panel of Figure 4 the new limits are shown in the $Y_P - D/H$ plane. For BBN only (no CMB constraints), in the absence of a light WIMP (EM or neutrino coupled), this pair of observables, $\{Y_P, D/H\}$, may be mapped exactly into the parameter pair, $\{N_{\text{eff}}, \Omega_B h^2\}$, as shown in the right hand panel of Fig. 4⁶. For BBN only, using the new D abundance,

$$\begin{aligned} \Delta N_\nu &= 0.50 \pm 0.23 \\ N_{\text{eff}} &= 3.56 \pm 0.23 \\ \eta_{10} &= 6.28 \pm 0.15 \quad (100 \Omega_B h^2 = 2.29 \pm 0.06). \end{aligned} \tag{9}$$

The current D and ^4He abundances favor neither standard big bang nucleosynthesis (SBBN: $\Delta N_\nu = 0$), nor the presence of a thermally equilibrated sterile neutrino ($\Delta N_\nu = 1$).

In the left hand panel of Figure 5 the independent BBN and CMB likelihood contours in the $N_{\text{eff}} - \Omega_B h^2$ plane are compared. The Planck results (those described by Eq. 74 of Ref. [2]) are adopted and are represented as shown in Table II of Ref. [1]. Despite the BBN contours having been displaced by the new D/H value to slightly higher $\Omega_B h^2$, there is still very good agreement between BBN and the CMB ($\chi^2 = 1.11$ with 2 degrees of freedom), justifying a joint BBN + CMB fit. The results of that joint fit are shown in the right hand panel of Fig. 5, where the 68.3% and

⁶ Because the BBN code used here employs the IND approximation, all figures show results consistent with using $N_{\text{eff}}^0 = 3.02$ as the numerical constant in Eqs. (7) and (8). When there is no light WIMP, it is a reasonable approximation to replace 3.02 by 3.05 and to include the related effect on Y_P as computed in Ref. [19] with $\Delta N_\nu = 0$. Accordingly, for the no-WIMP cases, we quote numerical results using $N_{\text{eff}}^0 = 3.05$ instead of 3.02 and have applied a small correction to the computed Y_P .

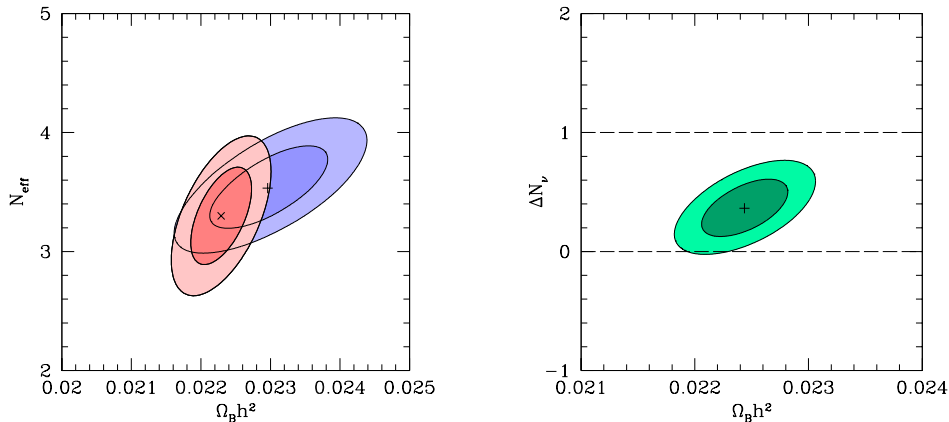


FIG. 5. (Color online) The left hand panel compares the BBN (upper right, blue contours) and CMB (lower left, pink contours) constraints in the $N_{\text{eff}} - \Omega_B h^2$ plane. The “x” shows the best fit CMB point and the “+” shows the best fit BBN point. In the right hand panel the joint BBN + CMB fit is shown in the $\Delta N_\nu - \Omega_B h^2$ plane. The “+” shows the best joint fit point, which is located at $\Delta N_\nu = 0.35$ and $\Omega_B h^2 = 0.0224$ (without resorting to the IND approximation).

95.5% contours are shown in the $\Delta N_\nu - \Omega_B h^2$ plane. The new, joint BBN + CMB fit, parameter values are

$$\begin{aligned} \Delta N_\nu &= 0.35 \pm 0.16 \\ N_{\text{eff}} &= 3.40 \pm 0.16 \\ \eta_{10} &= 6.15 \pm 0.07 \quad (100 \Omega_B h^2 = 2.24 \pm 0.03). \end{aligned} \tag{10}$$

Thus, while the new D abundance still allows $\Delta N_\nu = 0$ at 2.2σ ($\Delta N_\nu \geq 0$ is favored at $\gtrsim 98.8\%$ confidence), it strongly disfavors even one sterile neutrino, at $\sim 4.0\sigma$ ($\Delta N_\nu > 1$ excluded at $> 99.9\%$ confidence).

B. Constraints On New Physics Between BBN And Recombination

Since BBN is sensitive to physics when the Universe was a few minutes old, and the CMB probes physics some 400 thousand years later, the excellent agreement between the BBN and CMB constraints on the cosmological parameters explored here constrains at least some possibilities for “new physics” between these epochs in the early evolution of the Universe. If it is assumed that the “physics beyond the SM” that may arise between BBN and recombination can be described by the differences between the baryon to photon ratio ($\eta_B = 10^{-10}(n_B/n_\gamma)$) and ΔN_ν evaluated from BBN and the CMB, then their current agreement, within the errors, limits some classes of nonstandard physics. For example, if the baryon number is conserved in this interval, then the ratio $\eta_{10}^{\text{BBN}}/\eta_{10}^{\text{CMB}} = N_\gamma^{\text{CMB}}/N_\gamma^{\text{BBN}}$ probes the difference between the number of photons in a comoving volume at recombination (N_γ^{CMB}) compared to the number present at the end of BBN (N_γ^{BBN}). While entropy conservation suggests that $N_\gamma^{\text{CMB}}/N_\gamma^{\text{BBN}} \geq 1$, any deviation of this ratio from unity measures (limits) photon production (*e.g.*, from the decay or annihilation of a beyond the standard model particle) between these two, widely separated epochs. Since the standard models of particle physics and cosmology lack equivalent neutrinos, ΔN_ν probes any “extra” (beyond the SM) contribution to the early Universe radiation energy density (“dark radiation”) at BBN and at recombination (or, at the epoch of equal matter and radiation densities). A nonzero value of the change in ΔN_ν , $\delta(\Delta N_\nu) = \Delta N_\nu^{\text{BBN}} - \Delta N_\nu^{\text{CMB}}$, could also signal exotic, new physics. It is evident from Fig. 5 that both of these difference parameters, $\Delta N_\gamma/N_\gamma^{\text{BBN}} = N_\gamma^{\text{CMB}}/N_\gamma^{\text{BBN}} - 1$ and $\delta(\Delta N_\nu) = \Delta N_\nu^{\text{BBN}} - \Delta N_\nu^{\text{CMB}}$, are zero within the uncertainties. Fitting these two parameters results in $\Delta N_\gamma/N_\gamma^{\text{BBN}} = 0.027 \pm 0.026$ and $\delta(\Delta N_\nu) = 0.25 \pm 0.35$. Since we know that $\Delta N_\gamma \geq 0$, it probably makes more sense to compute an upper limit for $\Delta N_\gamma/N_\gamma^{\text{BBN}}$. The one-sided 95.5% limit (so that 4.5% of the likelihood lies at higher values) is $\Delta N_\gamma/N_\gamma^{\text{BBN}} < 0.072$. Notice that since the CMB displays a thermal spectrum, any photons produced after BBN must have been thermalized well before recombination. This has been assumed here. If thermalization occurred at redshift $5 \times 10^4 < z < 2 \times 10^6$ [31], this would have occurred at fixed photon number, and the CMB frequency spectrum would show a μ -distortion (nonzero chemical potential). There is a tight observational limit of $|\mu| < 9 \times 10^{-5}$ [32], strictly limiting the addition of photons at $z < 2 \times 10^6$.

C. Updated BBN And CMB Constraints On An EM Coupled Light WIMP

The new D abundance has a nearly negligible effect on the combined BBN and CMB parameter constraints for a light WIMP that annihilates to e^\pm pairs and/or photons in chemical equilibrium. The parameter constraints remain very nearly independent of the statistics obeyed by the WIMP (fermion or boson), with the largest variation among WIMP types occurring in the lower limits on the WIMP mass, from ~ 0.5 MeV for a real scalar WIMP to ~ 5 MeV for a Dirac fermion WIMP⁷. In light of the new data, the presence of a light EM coupled WIMP is still a good fit ($\chi^2 \sim 0.5$ for 1 degree of freedom) and remains slightly favored ($\Delta\chi^2 \sim 0.7$) over its absence; the best fit WIMP mass decreases from its previous value by $\lesssim 1$ MeV (*e.g.*, for a Majorana fermion WIMP, $\Delta m_\chi \approx -0.8$ MeV), while the $m_\chi \rightarrow \infty$ limit remains a good fit. For the other parameters, N_{eff} decreases slightly, from $N_{\text{eff}} = 3.30 \pm 0.26$ to $N_{\text{eff}} = 3.22 \pm 0.25$, and ΔN_ν is virtually unchanged, $\Delta N_\nu = 0.65^{+0.45}_{-0.37}$. The lower limits on the WIMP masses are loosened by only ~ 0.2 MeV for Majorana and ~ 0.3 MeV for Dirac WIMPs⁸.

IV. BBN IN THE PRESENCE OF A NEUTRINO COUPLED LIGHT WIMP

A. Physical effects

For BBN, the case considered here, of an equilibrated light WIMP that couples only to neutrinos, is in some ways the opposite of the case examined in Ref. [1], where the light WIMP coupled to the electromagnetic plasma. In both cases, the light WIMP speeds up expansion at very early times by contributing directly to the energy density. As the temperature drops and the WIMP becomes nonrelativistic, the entropy of a neutrino-coupled WIMP is transferred to the neutrinos, giving them a higher temperature at fixed T_γ than in the standard model. This ensures that the expansion rate (again, at fixed T_γ) is faster than in the standard model. In addition, in this case the neutrino heating skews the weak interactions interconverting protons and neutrons, because hotter neutrinos more easily supply the Q -value to make a neutron and a positron from a proton. These effects, linked to neutrino temperature, are the opposite of the electromagnetically coupled case.

The effects on the expansion rate are shown in Fig. 6, in which the expansion timescale (comparable to the age of the universe) is shown as a function of T_γ for Majorana WIMPs of several masses, assuming that neutrinos decouple suddenly from the EM plasma at $T_{\nu d} = 2$ MeV. Since the timescale is shown normalized to its value, t_{SM} , at the same T_γ in the standard model, values below unity reflect expansion that has been sped up by the light WIMP. A 10 MeV WIMP (the highest mass shown) contributes some energy density of its own to the expansion rate at early times but quickly transfers that energy to the neutrinos. As the WIMP mass decreases, more of its entropy ends up being carried by neutrinos, but the transfer happens later. WIMPs with $m_\chi \lesssim T_{\nu d}$ contribute initially as a relativistic species, equivalent to a unit increment of ΔN_ν if the WIMP is Majorana; this limit is shown as the second-highest dashed line in Fig. 6. Once the WIMPs and the electrons and positrons have all annihilated, a Majorana WIMP has heated the neutrinos so that the expansion rate is about 8% faster than in the standard model – this limit is the second-lowest dashed line in Fig. 6. If $m_\chi \lesssim m_e$, there is an intermediate time at $T_\gamma \lesssim m_e$ when electrons and positrons have annihilated but WIMPs have not. In Fig. 6 this is visible as a rise in timescale (slower expansion) toward a limit that remains about 6% faster than standard-model expansion. The temperature range covered by this rise is exactly the range where the deuterium and lithium abundances are determined, late in BBN; it will be shown below that this results in a reversal of the general trend of abundances as functions of m_χ .

One effect found in the electromagnetically coupled case has no analogue here: the annihilation of an EM coupled WIMP ultimately produces photons, changing the baryon to photon ratio η . WIMP annihilation to photons after e^\pm annihilation (especially if it happens after BBN ends) produces large shifts in the BBN yields at fixed late-time η , and this dominates much of the BBN results in Ref. [1]. The effects on BBN of a neutrino-coupled light WIMP therefore tend to be generally smaller than those of an EM coupled light WIMP.

B. BBN calculations

The effects described above have been included in BBN calculations using a modified version of the Kawano BBN code [34, 35], assuming IND at $T_{\nu d} = 2$ MeV. With the exception of adding neutrino coupled WIMPs (and setting the

⁷ As noted in [1], the variation in the best fit mass values is much smaller, ranging from ~ 5 MeV for a real scalar to ~ 10 MeV for a Dirac fermion.

⁸ We note that the previous paper suffered from an error that placed the lower limits on m_χ at 96% confidence rather than 95.5%, so that the tabulated limits were 0.1 to 0.2 MeV lower than intended. The further correction due to the revised D/H is independent of this and in the opposite direction, so that the revised D/H mainly cancels the mistake.

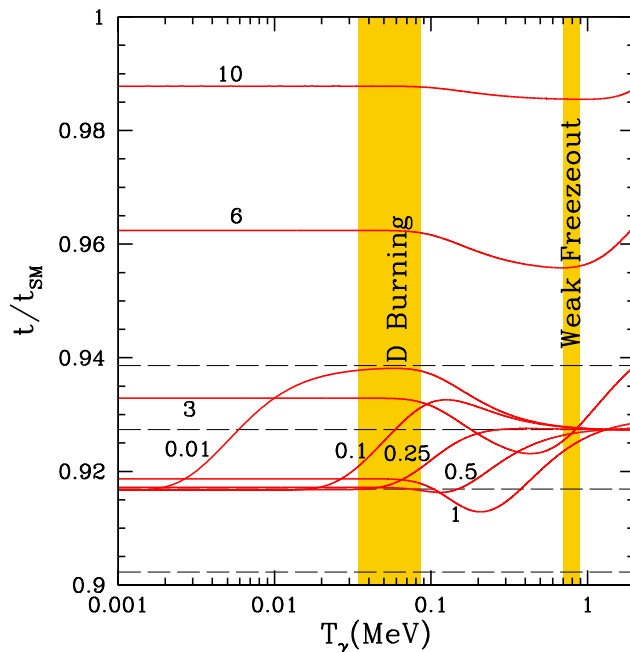


FIG. 6. (Color online) The expansion timescale (reciprocal of the logarithmic time derivative of the scale factor) is shown as a function of the photon temperature (T_γ) for several values of the mass (m_χ) of a light Majorana WIMP. Timescales are shown in units of t_{SM} , the timescale at the same T_γ in the standard model. Curves are labeled by m_χ in MeV. Vertical bands indicate the temperatures at which weak freezeout of the nucleons and final burning of deuterium (and production of lithium) occur. From top to bottom, horizontal dashed lines indicate limits in which e^\pm have annihilated but WIMPs have not; e^\pm and WIMPs are both fully relativistic; e^\pm and WIMPs have fully annihilated; and WIMPs have annihilated fully but the e^\pm pairs have not. The bottom dashed line is not reached because m_e and $T_{\nu d}$ are so close that it is not possible for WIMPs of any mass to go from the relativistic limit at neutrino decoupling to fully annihilated before e^\pm annihilation.

g -factor of EM coupled WIMPs to zero), the code is as described in Ref. [1]. The interested reader is referred there for computational details. Two details that are particularly important for the present results (though unchanged from the previous calculation) are mentioned here, before discussion of the new modifications.

The present results are based on a neutron lifetime of $\tau_n = 880.1 \pm 1.1$ s (with this error propagated through the analysis), as recommended by the Particle Data Group in 2012 [36], though the recommended lifetime has now been revised to 880.3 ± 1.1 s after reanalysis of three experiments [37]. Since this shift is smaller than the error estimate, and changing τ_n would produce confusing inconsistencies with our earlier work, we use the older value here. Both τ_n values are averages of discrepant data (with inflated error bars to reflect this); we hope that the disagreement will be resolved by the next generation of experimental results. One indication of how far the results might shift is given by the current difference between the two experimental approaches, with the mean τ_n from “bottle” methods being near the value used here and that from “beam” methods being larger by about 8 seconds [38]. This 8 second difference corresponds to about the same effect on BBN predictions of Y_P as a change of -0.13 in ΔN_ν , so the main effect of even a drastically longer lifetime (for fixed Y_P) would likely be to reduce the fitted N_{eff} and ΔN_ν values by about this amount. This shift is about half the size of the quoted 1σ uncertainties of these parameters, *e.g.* in § III.

Another important detail is the rate for the deuterium-destroying reaction $d(p, \gamma)^3\text{He}$. Most calculations incorporate an empirically-derived cross section [39, 40] for this process, which depends on a single experiment at the most important energies for BBN. The calculations here are based on an *ab initio* calculation of the cross section [41, 42], which is likely to be more reliable (with a 7% error assigned and propagated through our analysis) [43]. The difference amounts to about a 5% lower predicted D/H at fixed parameters here compared to much of the recent literature, and thus a roughly 3% shift in the BBN inferred baryon mass density parameter, $\Omega_B h^2$. Since there is good agreement between D/H and the CMB in Sec. III A, the empirical rate implies tension between BBN and the CMB at about the 90% confidence level when the empirical rate is used, as found in Refs. [44, 45]. Use of the empirical rate shifts ΔN_ν downward by about 0.02 in the absence of CMB constraints. In joint BBN and CMB fitting, ΔN_ν and N_{eff} shift downward by about 0.1, allowing $\Delta N_\nu = 0$ at 95% confidence, while the lower bounds on m_χ tighten by about 10%. Further experimental and theoretical work on this cross section in the 50 – 500 keV energy range is highly desirable.

Incorporation of a neutrino-coupled WIMP into the code required first promoting T_ν to a dynamic variable. In the original Kawano code, the neutrino temperature used in the weak rates is computed from the baryon density, using the proportionality of both quantities to the cube of the expansion scale factor. This works because the Kawano code assumes IND and starts after neutrino decoupling, so the neutrino energies simply redshift with the expansion of the Universe.

With the addition of neutrino-coupled WIMPs, T_ν satisfies a differential equation that must be solved simultaneously with that for the expansion, just like T_γ . Where the T_γ equation has terms for photon and e^\pm entropies, the T_ν equation has terms for neutrino and light WIMP entropies. Since the WIMPs are assumed to be in equilibrium with the SM neutrinos, they share the same temperature. The energy density of equivalent neutrinos is computed from its scaling with the baryon density just as before. If the light WIMPs are in equilibrium with all neutrino species (as in Eq. (8)), this can be accounted for by adjusting the spin-degeneracy factor of the “SM neutrino” term in the T_ν equation so that the total energy density of neutrinos is $(3 + \Delta N_\nu)\rho_\nu$, and setting the equivalent-neutrino density variable in the code to zero. As mentioned above, we assumed even in this latter case that ΔN_ν can take on any value, so that the corresponding neutrino spin-degeneracy factor need not be an integer.

The results of the BBN calculations including neutrino-coupled WIMPs are shown for all four WIMP spin-statistics possibilities considered and for $\Delta N_\nu = 0$ in Figs. 7 and 8. The overall scale of a light WIMP’s effects is smaller than in the corresponding figures of Ref. [1], where we considered an EM coupled WIMP. These results are in good agreement with previously published calculations [3, 4, 18, 21]. The programming error suggested [1] as a possible explanation of the difference between Refs. [1] and [4] for EM coupled WIMPs, does not affect the calculations for neutrino-coupled WIMPs.

The results for D, ^3He , and ^7Li in Fig. 7 can be understood entirely from the timescales shown in Fig. 6. For $m_\chi \gtrsim 30$ MeV, the WIMP annihilates before neutrino decoupling and has no effect on the ratio of neutrino and photon temperatures. For lower m_χ , the WIMP energy density initially contributes to the expansion rate and then raises T_ν/T_γ relative to the SM. This causes expansion at fixed T_γ to be faster, including at $T_\gamma \sim 50$ keV when the D, ^3He , and ^7Li abundances are determined. Since D and ^3He are being burned at the end of BBN, faster expansion implies less time to burn them away, leading to higher relic abundances. The ^7Be precursor of ^7Li is still being produced at the end of BBN, so faster expansion implies less time for its production and therefore results in a lower relic ^7Li abundance.

If the WIMPs are so light that they do not annihilate away until after BBN, their effect is smaller. Annihilation of e^\pm and the corresponding heating of photons always occur before BBN stops, and if the WIMPs are still present, the result is slower expansion at given T_γ than if the WIMPs had already annihilated. This decreases the size of the speed-up effect, so that at very low m_χ (the left sides of the graphs in Fig. 7) the yield curves trend back towards the $m_\chi \rightarrow \infty$ limit.

The helium evolution story is more complicated, as was also true for EM coupled WIMPs [1]. The BBN predicted helium abundance shows effects both from the expansion timescales and from the influence of the hotter neutrinos on the weak rates. In the EM coupled case the changes in Y_P produced by these effects had opposite signs and partially cancelled, though they had different m_χ dependences. Here they all push Y_P higher, so the deviation from the $m_\chi \rightarrow \infty$ limit has the same sign at all m_χ in Fig. 7. However, neutrino-coupled WIMPs cannot shift η , so the maximum size of the shift in Y_P is not as large for neutrino coupled as for EM coupled WIMPs.

As discussed in Ref. [1], the ^3He and ^7Li abundances are of less interest for the analysis presented here than are the D and ^4He abundances. In the case of ^3He , this is because of the difficulty of observing primordial ^3He directly and the apparently complicated chemical evolution that produced the $^3\text{He}/\text{H}$ observed in the Galaxy at roughly solar metallicities [46]. Lithium suffers from the well-known “BBN lithium problem”: the lithium abundance (Li/H) inferred from observations of low-metallicity stars is lower than the SBBN prediction by a factor $\gtrsim 3$ [49, 50]. The models considered here cannot produce a downward shift of Li/H of comparable size for any choice of parameters. Moreover, we will see below that once these parameters are fixed to reproduce the observed deuterium and helium abundances, the lithium yield is essentially fixed at its SBBN value. Whatever is wrong with lithium, it cannot be solved by the light WIMP scenario. A similar result was found for EM coupled WIMPs [1] (and also in the absence of any light WIMP) and is driven by the anticorrelation between the BBN predicted D and Li abundances.

We now examine the results of the BBN calculations for $\Delta N_\nu = 0$ (no equivalent neutrinos) and varying WIMP mass shown in Fig. 8 in the $Y_P - \text{D}/\text{H}$ plane. The contours corresponding to the Cooke et al. [25] D/H constraint and the Izotov et al. 2013 [27] Y_P constraint are shown in Fig. 8, just as in Fig. 4. The baryon density has been fixed (at the Planck ΛCDM value) and the WIMP masses varied between 40 MeV and 4 keV as in Fig. 7. Starting from the SBBN limit, $m_\chi \rightarrow \infty$, each curve proceeds toward higher yields of both nuclides. There is a change in slopes near $m_\chi = 3$ MeV, corresponding to changes in the slope of both yields as functions of m_χ seen in Fig. 7. Around $m_\chi = 200$ keV, the decline of each curve away from its maximum in Fig. 7 manifests itself as a sharp hook in Fig. 8. Finally, each curve ends at a limiting $m_\chi \rightarrow 0$ point. At this limiting point, the very light WIMP is indistinguishable (for BBN) from an equivalent neutrino: it remains relativistic all the way through BBN. Thus, for

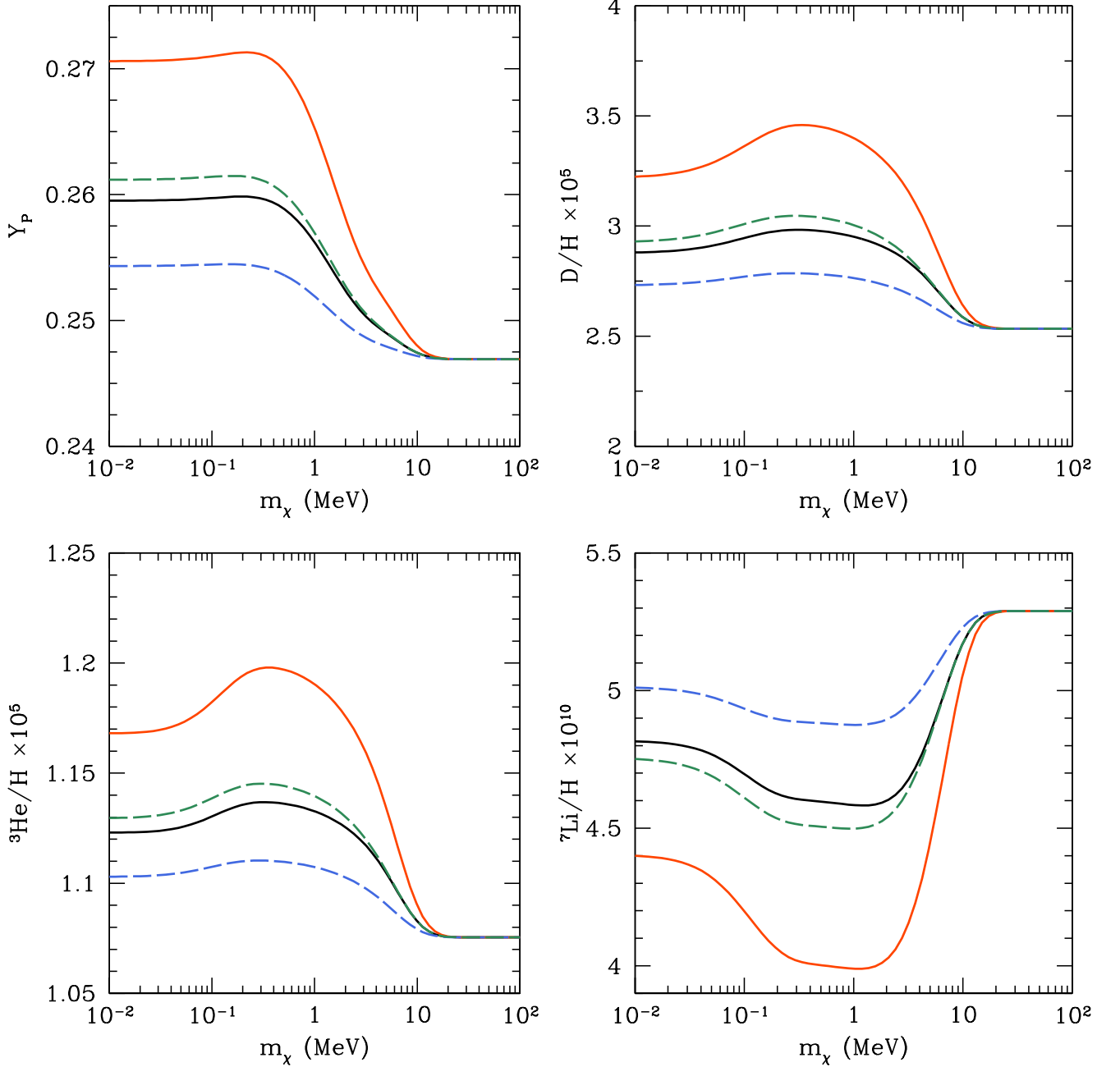


FIG. 7. (Color online) For the case of a light WIMP that annihilates to the SM neutrinos, the four panels show the BBN yields of ${}^4\text{He}$ (upper left), D (upper right), ${}^3\text{He}$ (lower left), and ${}^7\text{Li}$ (lower right) as functions of the WIMP mass, m_χ , for $\Omega_B h^2 = 0.0220$ and $\Delta N_\nu = 0$. Solid curves show results for fermionic WIMPs (red for Dirac, black for Majorana) and dashed curves for bosonic WIMPs (green for a complex scalar, blue for a real scalar). The sequence of curves is Dirac, complex scalar, Majorana, and real scalar, from top down in all panels except the lower right, where it is reversed. The ${}^4\text{He}$ abundance is shown as a mass fraction Y_P , and the other abundances are shown as ratios by number to hydrogen.

a Majorana WIMP this final limiting point corresponds to $m_\chi > 30$ MeV and $\Delta N_\nu = 1$, and consequently it lies on the (short-dashed) curve of infinite m_χ and varying ΔN_ν . BBN alone cannot distinguish between the parameter pairs $(m_\chi > 30 \text{ MeV}, \Delta N_\nu = 1)$ and $(m_\chi = 0, \Delta N_\nu = 0)$ for a Majorana WIMP. It is evident from Fig. 2 that the CMB does not share this degeneracy. For the other WIMP types considered here, ΔN_ν is incremented not by one unit but by $4/7$ (real scalar), $8/7$ (complex scalar), or 2 (Dirac). The equivalence of low m_χ and higher ΔN_ν is also evident in Fig. 13, considered below.

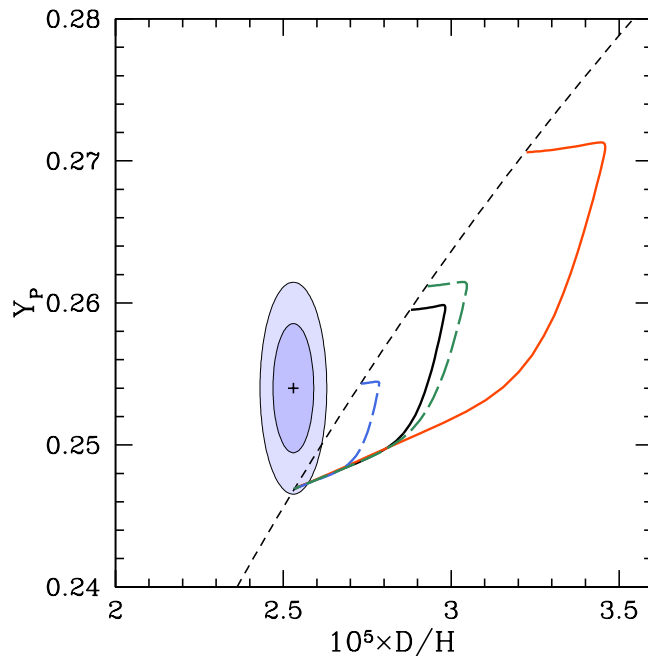


FIG. 8. (Color online) Yield curves for the ${}^4\text{He}$ mass fraction, Y_{P} , and the deuterium abundance, $y_{\text{DP}} = 10^5(\text{D}/\text{H})_{\text{DP}}$, for $\Delta N_{\nu} = 0$ and fixed $\Omega_{\text{B}}h^2 = 0.0220$, for the four types of neutrino coupled WIMPs considered here: real and complex scalars (long-dashed curves, from left to right) and Majorana and Dirac fermions (solid curves, from left to right); colors as in Fig. 7. The WIMP mass decreases along the curves from the lower left (high mass, the no light WIMP limit) to the upper right (very light WIMP). The short-dashed curve shows the no-WIMP limit at varying ΔN_{ν} ; the other curves each touch this limiting curve at both ends because a WIMP with $m_{\chi} \ll m_e$ is equivalent (for BBN) to a heavy WIMP (no light WIMP) with an incremented value of ΔN_{ν} . The 68.3% and 95.5% contours for the D and ${}^4\text{He}$ primordial abundances adopted here are also shown.

The BBN equivalence of very low m_{χ} and increased ΔN_{ν} , combined with the shape of the curves in Fig. 8, implies that it is difficult for neutrino coupled light WIMPs to produce BBN yields that are very different from a model where ΔN_{ν} and $\Omega_{\text{B}}h^2$ are the only free parameters. At fixed $\Omega_{\text{B}}h^2$, the yields with varying WIMP mass stay close to the curve of varying ΔN_{ν} , with the extremes of m_{χ} lying on that curve. The farthest distance from the curve of varying ΔN_{ν} occurs at the shallow bend seen in the curves of Fig. 8, so large changes in m_{χ} are degenerate with relatively modest changes in $\Omega_{\text{B}}h^2$ and ΔN_{ν} .

C. Parameter constraints from BBN alone

The three panels of Figure 9 show the results of employing the BBN results discussed above, for a neutrino coupled Majorana WIMP, to constrain the cosmological parameters. For each value of the WIMP mass there is always a pair of η_{10} and ΔN_{ν} (or equivalently $\Omega_{\text{B}}h^2$ and N_{eff}) values such that the BBN yields for D and ${}^4\text{He}$ agree with their observationally inferred abundances. This is shown by the solid (black) curves in Fig. 9; the darker/lighter (blue) bands are 68.3% and 95.5% frequentist intervals in these parameter values, computed using profile likelihoods [36, 48]. The contours shown in the left and middle panels of Fig. 9 are the BBN constraints on ΔN_{ν} and $\Omega_{\text{B}}h^2$ from D and ${}^4\text{He}$, as functions of the WIMP mass. In the right hand panel of Fig. 9 the information from the left and middle panels is projected onto the $\Omega_{\text{B}}h^2 - \Delta N_{\nu}$ plane, so that m_{χ} is eliminated. The solid (black) curve in this panel shows the locus of exact fits, which vary with WIMP mass.

The results for ΔN_{ν} as a function of m_{χ} shown in the left hand panel of Fig. 9 can be understood with reference to the two upper panels of Fig. 7. As shown in § III A, the observationally inferred primordial helium and deuterium abundances, Y_{P} and $y_{\text{DP}} \equiv 10^5(\text{D}/\text{H})_{\text{P}}$, can be fitted simultaneously with $\Delta N_{\nu} \approx 0.5$ and $\Omega_{\text{B}}h^2 \sim 0.022$. Starting from this fit and reducing m_{χ} from infinity ($\gtrsim 30$ MeV), the predicted values of Y_{P} and y_{DP} both increase, so ΔN_{ν} and $\Omega_{\text{B}}h^2$ must be refitted. The helium abundance is relatively insensitive to changes in the baryon density, but it is quite sensitive to changes in ΔN_{ν} . At low WIMP mass, $m_{\chi} \lesssim 10$ MeV, the BBN predicted helium abundance can be restored to consistency with the observed abundance by reducing ΔN_{ν} . At very low m_{χ} , a Majorana WIMP affects

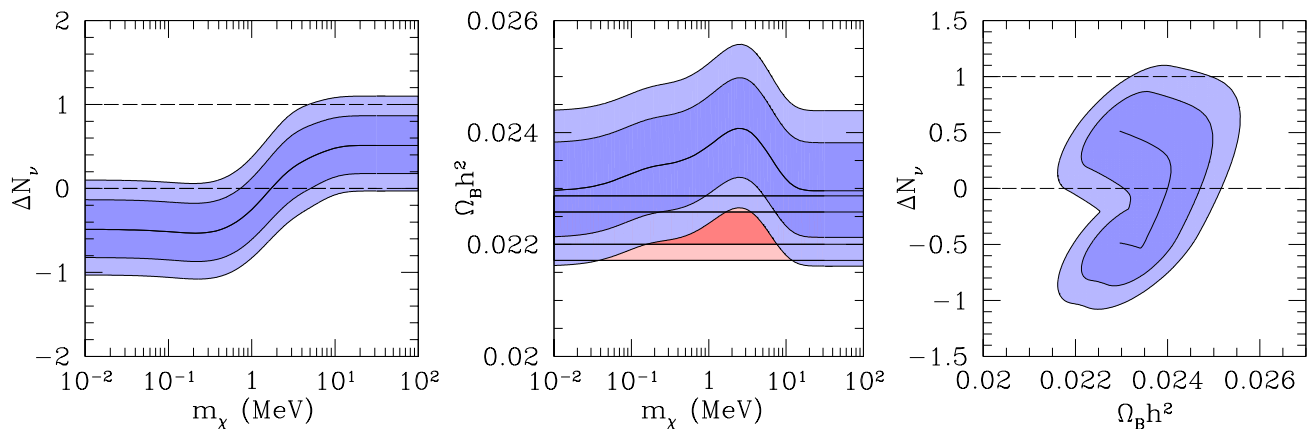


FIG. 9. (Color online) The left panel shows ΔN_ν and the middle panel shows $\Omega_B h^2$ as functions of the WIMP mass for a Majorana fermion WIMP that annihilates to SM neutrinos. The horizontal (red/pink) bands in the middle panel show, for comparison, the CMB constraints on $\Omega_B h^2$ (that are independent of the WIMP mass). The right panel shows the 68.3% and 95.5% contours for the BBN constraints in the $\Delta N_\nu - \Omega_B h^2$ plane that follow from the left and middle panels. Darker and lighter blue (curved) contours show the BBN determined 68.3% and 95.5% confidence level regions of the joint likelihoods for each pair of parameters, using as constraints only D/H and Y_P . The solid (black) curve running through the middle of these regions shows the BBN best fit parameter values at each m_χ value. (In the right panel, this curve runs from high m_χ at the top end of the curve – which is the best-fit point in Fig. 4 – to low m_χ at the bottom end.) In the left and right hand panels the dashed lines show $\Delta N_\nu = 0$ and 1 as guides to the eye. Note that the curve in the left-hand panel has the same shape (after up-down reflection) as the curve in the upper left panel of Fig. 7, reflecting the role of Y_P in fitting this parameter.

Y_P in exactly the same way as a sterile neutrino, so the best fit at very low mass is one unit of ΔN_ν lower than the best fit for $m_\chi > 30$ MeV. In fact, the curve of ΔN_ν vs. m_χ in Fig. 9 is very nearly the curve of Y_P vs. m_χ in Fig. 7, flipped upside down.

Lowering ΔN_ν also lowers y_{DP} , helping to reconcile it with a light WIMP, but the ΔN_ν that fits Y_P is not low enough to bring y_{DP} back into full agreement. Deuterium is more sensitive than Y_P to $\Omega_B h^2$, which can be increased to further reduce y_{DP} into agreement with the data. This is visible in the middle panel of Fig. 9 in the mass range $\sim 1 - 10$ MeV. Just as for Y_P , low WIMP masses ($\lesssim 0.1$ MeV) can be compensated in y_{DP} exactly by a unit decrease of ΔN_ν , so the $\Omega_B h^2$ that provided the exact fit at high m_χ is also the best fit at low m_χ . This is also visible in the middle panel of Fig. 9.

In carrying out our calculations, we have permitted $\Delta N_\nu < 0$ by allowing for negative values of the equivalent neutrino energy density (though the sum of SM and equivalent neutrino energy densities remains positive). Especially in the BBN-only analysis, this is allowed formally by the observational data. However, since there are known to be three standard-model neutrino species, $\Delta N_\nu < 0$ cannot be achieved by adding new species as contemplated here, and it is unphysical without further assumptions. There are two ways to address this issue. We could impose directly an *a priori* constraint that $\Delta N_\nu \geq 0$. Alternatively, we could use the CMB (Planck) constraint on N_{eff} [2] and the assumption that $\Delta N_\nu \geq 0$ to set a lower limit on m_χ , and then fit the parameters without imposing a sharp limit on ΔN_ν . We have done both and find that the parameter constraints in the two approaches are essentially equivalent (unless the WIMP is a real scalar, which affects the CMB too little for this approach to work). Next, in § V, we describe the results of the joint CMB + BBN analysis. The merits of imposing the cut on m_χ instead of directly on ΔN_ν will be evident there.

V. JOINT BBN AND CMB CONSTRAINTS ON A NEUTRINO COUPLED WIMP

The upper set of curves in Fig. 1 shows, for neutrino coupled WIMPs, N_{eff}^0 as a function of the WIMP mass, where N_{eff}^0 is the value of N_{eff} when $\Delta N_\nu = 0$. In comparison with the Planck constraint on N_{eff} [2], it is clear that at low WIMP mass, consistency with the CMB requires $\Delta N_\nu < 0$ (though the requirement is weak if the WIMP is a real scalar). This is shown in Figure 10, where the fitted $\Delta N_\nu \approx N_{\text{eff}}(\text{Planck}) - N_{\text{eff}}^0$ (cf. Eq. 7) is shown as a function of the WIMP mass, for a Majorana fermion WIMP. Comparing this result with those of the previous section, we see that in the low mass limit, both the CMB and BBN require $\Delta N_\nu < 0$ to accommodate very light neutrino coupled WIMPs. The joint BBN and CMB constraints can be used to separate the unphysical, $\Delta N_\nu < 0$ mass range, from

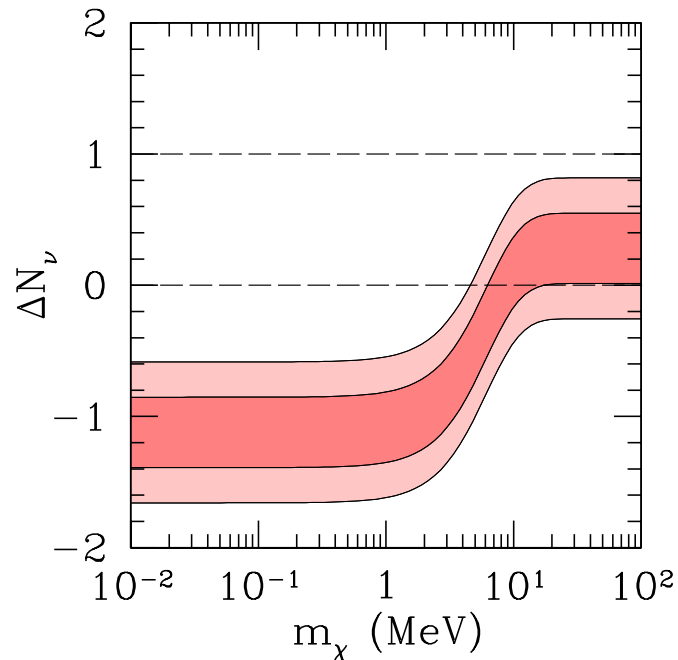


FIG. 10. (Color online) ΔN_ν as a function of the (Majorana) WIMP mass, showing 68.3% and 95.5% confidence limits inferred from the Planck CMB data (Eq. 74 of Ref. [2]) and Eq. 7 ($\Delta N_\nu \approx N_{\text{eff}}(\text{CMB}) - N_{\text{eff}}^0(m_\chi)$).

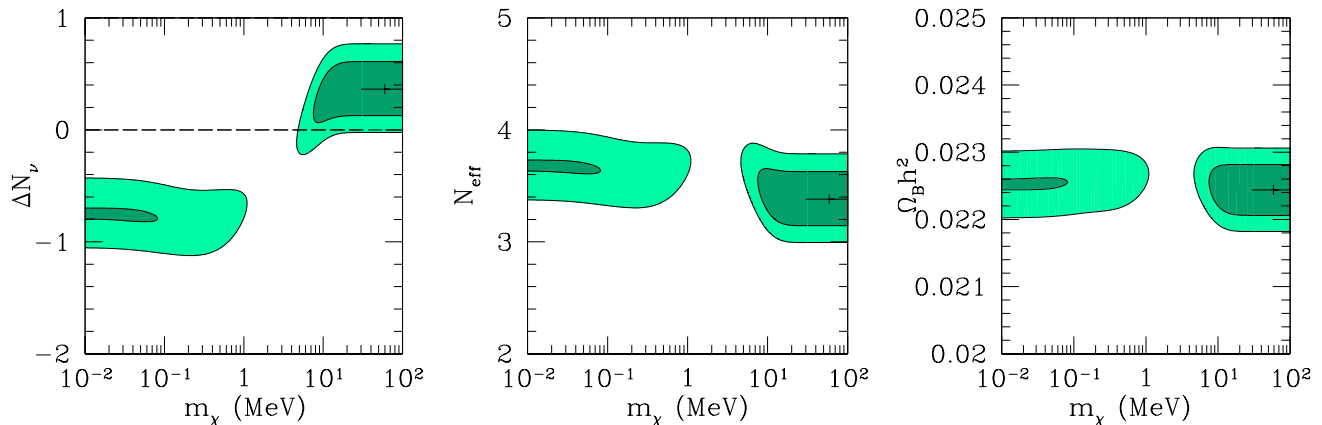


FIG. 11. (Color online) The joint BBN + CMB two-parameter 68.3% and 95.5% confidence contours of m_χ and ΔN_ν (left panel), N_{eff} (middle panel), and $\Omega_B h^2$ (right panel). Results are shown for a Majorana WIMP that annihilates to SM neutrinos. The “+” shows the best fit point in the parameter space, which is within $\Delta\chi^2 = 10^{-4}$ of $m_\chi \rightarrow \infty$. In the left hand panel the dashed line shows $\Delta N_\nu = 0$ as a guide to the eye. Since these contours indicate the joint constraints on two parameters, they correspond to different χ^2 values than would the boundaries on the single parameters in Eqs. (11) and (12).

the mass range where $\Delta N_\nu \gtrsim 0$. This is illustrated for Majorana WIMPs in Figure 11, where the left hand panel shows the joint BBN + CMB best fit and 68.3% and 95.5% simultaneous constraints on ΔN_ν and m_χ , and the right hand panel shows simultaneous constraints on $\Omega_B h^2$ and m_χ . (Likelihoods involving the CMB constraints are again computed as in § III.) As is revealed by these figures, there are two “peninsulas” of acceptable fits to the combined BBN and CMB data, separated by a region of very low likelihood. One is located at relatively high WIMP mass ($m_\chi \gtrsim 5$ MeV) corresponding to $\Delta N_\nu \gtrsim 0$ and with minimum $\chi^2 \sim 1.2$ (1 degree of freedom), while the other is at low WIMP mass ($m_\chi \lesssim 1$ MeV), corresponding to $\Delta N_\nu < 0$ and larger minimum χ^2 (1.8 for real scalars, 3.3 for Majorana fermions, and 10.2 for Dirac fermions). Examination of Figs. 10 and 11 indicates that the physical regime where $\Delta N_\nu \geq 0$ occurs only where $m_\chi \gtrsim 2$ MeV, so we restrict our analysis to $m_\chi > 2$ MeV in order to isolate the

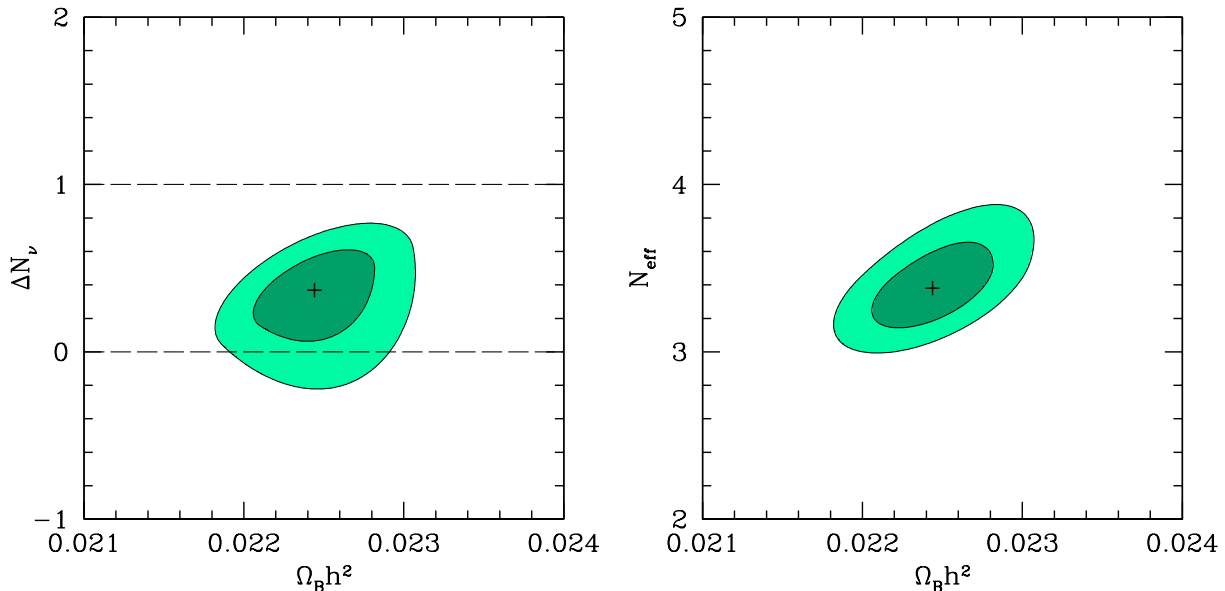


FIG. 12. (Color online) Two-parameter joint contours of ΔN_ν (left panel) and N_{eff} (right panel) with the baryon mass density ($\Omega_B h^2$) for a Majorana fermion WIMP that annihilates to SM neutrinos. Limits were determined by joint BBN + CMB fitting with the restriction that $m_\chi \gtrsim 2$ MeV (see the text). The “+” shows the best fit point in each panel. In the left hand panel the dashed lines show $\Delta N_\nu = 0$ and 1 as guides to the eye.

high- m_χ peninsula in the fitting, unless otherwise stated. Having ruled out the “peninsula” at low m_χ in this way, we arrive at the simultaneous constraints for ΔN_ν , N_{eff} , and baryon density ($\Omega_B h^2$) shown in Fig. 12, and the lower limits on m_χ shown in Table I.

The best fit point is at $m_\chi \gtrsim 35$ MeV, which is in the $\Delta N_\nu \geq 0$ regime, and is essentially at the limit of no light WIMP⁹. For all types of neutrino coupled WIMPs, the preferred parameter values and their 1σ ranges are very close to those in Eq. (10) for no light WIMP at all:

$$\begin{aligned} \Delta N_\nu &= 0.37^{+0.16}_{-0.17} \\ N_{\text{eff}} &= 3.38^{+0.17}_{-0.16} \\ 100 \Omega_B h^2 &= 2.24 \pm 0.03 \end{aligned} \quad (11)$$

The difference in the best-fit parameters between these results and those in Eq. (10) lies entirely in the corrections to the IND approximation included in the earlier analysis; we did not attempt such a correction when including light WIMPs. In Fig. 12, the contours can be seen as simple ellipses centered on the high- m_χ best fit from Fig. 5, superimposed with regions allowed by the dip in ΔN_ν at $m_\chi \lesssim 10$ MeV in Fig. 11. This allowed region of slightly lowered m_χ introduces the asymmetry seen at 1σ in Eq. (11), rendering the projection of the likelihoods onto the ΔN_ν axis non-Gaussian; multiples of the 1σ error are poor guides to the tails of the distribution. In particular, having isolated high- m_χ contours only by restricting the WIMP mass to $m_\chi > 2$ MeV, we still obtain a small region allowed at 95.5% confidence where $\Delta N_\nu < 0$. Boundaries of 95.5% confidence in single parameters (ignoring $\Omega_B h^2$, which does not deviate significantly from Gaussian likelihood) are

$$\begin{aligned} \Delta N_\nu &= 0.37^{+0.32}_{-0.44} \\ N_{\text{eff}} &= 3.38^{+0.38}_{-0.31}. \end{aligned} \quad (12)$$

For a real scalar WIMP, there is no way to isolate the high- m_χ likelihood minimum at a level that matters for the limits presented here. This is because it is possible to traverse the region between the “peninsulas” in Fig. 11

⁹ For all cases except for real scalar WIMPs, a formal best fit was found at $m_\chi \approx 35$ MeV, though this is only better than the $m_\chi \rightarrow \infty$ limit by $\Delta\chi^2 \sim 10^{-4}$. This corresponds to tiny differences in the computed quantities, smaller than the precision of both the data constraints and the underlying inputs such as nuclear rates; it is comparable to the precision of the interpolation table used to provide BBN outputs for the likelihood calculation.

TABLE I. Joint BBN+CMB lower limits on the mass of a neutrino coupled WIMP for WIMPs with the different spin degeneracies indicated. These are one-sided 95.5% limits, so that 4.5% of the likelihood lies at lower m_χ . The CMB constraints on $\Omega_B h^2$ and N_{eff} in the first line are from the Planck $\Lambda\text{CDM} + N_{\text{eff}}$ fit including BAO (Eq. 74 of Ref. [2]). In the second line, the Planck fit includes Y_P as a fitted parameter (Eq. 89 of Ref. [2]), and this constraint on Y_P is included in our fit. The correlations between Planck parameters have been included as described in Ref. [1].

Inputs	Minimum m_χ (MeV)			
	Real scalar	Majorana	Complex scalar	Dirac
BBN+Planck $\Lambda\text{CDM} + N_{\text{eff}}$	4.16	6.93	6.98	9.28
BBN+Planck $\Lambda\text{CDM} + N_{\text{eff}} + Y_P$	^a –	6.68	6.74	9.07

^a No value of m_χ is ruled out at 95.5% significance.

without passing through a point where $\Delta\chi^2 \geq 4$ (relative to the global best fit), and also because the local minimum of χ^2 in the low- m_χ regime has $\Delta\chi^2 < 1$. Requiring that $\Delta N_\nu \geq 0$ for real scalars, it is possible to obtain a weak lower limit on m_χ (Table I), and the 95.5% (two-sided) upper limit on N_{eff} becomes 3.83. Limits are otherwise the same as in the other cases. As in the absence of a light WIMP (but not the presence an EM coupled WIMP), a sterile neutrino ($\Delta N_\nu = 1$) is strongly disfavored, at more than 99% confidence, in the presence of a neutrino coupled WIMP. However, the complete absence of equivalent neutrinos is also disfavored in all cases, but “only” at the $\sim 98\%$ confidence level.

As described in §II A and §IV B, there exist the two possibilities that the light WIMP couples only to the SM neutrinos (resulting in Eq. (7)) and that it couples to both SM and equivalent neutrinos (resulting in Eq. (8)). The results quoted here were all computed for coupling only to SM neutrinos, which would seem to be the physically more interesting case. Within the precision of rounding, the same results as Eqs. (11) and (12) are found in the other case, provided that ΔN_ν is still permitted to vary continuously, and mass limits within 200 keV of those in Table I result. The two sets of results are guaranteed to be close by the location of the best fit at $m_\chi \rightarrow \infty$, the small allowed values of ΔN_ν , and the passage of the BBN-only best fit curve (Fig. 9) through $\Delta N_\nu = 0$; as discussed in §IV B above, there is no difference between the two possibilities when $m_\chi \rightarrow \infty$ or $\Delta N_\nu = 0$, so results for the two cases never get very far apart.

A. Lower Bound To The Mass Of A Neutrino Coupled Light WIMP

The lower bound to the mass of a neutrino coupled WIMP is of interest for limits on possible dark matter masses and elastic cross sections [51–53]. The lower bounds to the mass of a neutrino coupled light WIMP derived from our joint BBN+CMB analysis are presented in Table I. It is important to consider whether the limits on m_χ in Table I truly rule out all lower masses, or if there is some mass below which our analysis no longer applies. In the BBN calculation it is assumed that the light WIMP remains coupled to the SM neutrinos during BBN, but not necessarily after BBN has ended. If this were not true, and WIMPs decoupled when still relativistic during or before BBN, the relic number density of light WIMPs today would be similar to that of the SM neutrinos. In this case, any m_χ greater than a few eV would contribute too much to the cold, warm, or hot mass density in the present universe. Thus, any WIMP massive enough to annihilate during or before BBN must have annihilated then, and any lighter WIMP remains coupled to the SM neutrinos all the way through BBN, as assumed in the analysis here. From Fig. 9 and analogous calculations for other WIMP types, BBN alone, along with the requirement that $\Delta N_\nu \geq 0$, forbids all $m_\chi < 600$ keV (800 keV, 2.1 MeV) for a Majorana WIMP (complex scalar WIMP, Dirac WIMP), without exception. At the 95.5% confidence level, the BBN constraint alone does not forbid a real scalar WIMP of any mass.

For the joint BBN+CMB limit on m_χ from the analysis presented here to be valid, it is also necessary that the relation between m_χ and N_{eff}^0 shown in Fig. 1 holds. This requires that the light WIMP remain in equilibrium with the SM neutrinos until after it has annihilated (at $T_\nu \sim m_\chi/3$), in order that $n_\chi/n_\nu \ll 1$ well before recombination. Thus, as mentioned above, any neutrino coupled WIMP with mass greater than a few eV must have annihilated prior to recombination (or, prior to the epoch of equal matter-radiation densities), heating the SM neutrinos as assumed in the joint BBN+CMB analysis here.

A light WIMP that is still relativistic after recombination ($m_\chi \lesssim 0.1$ eV) should count in the CMB as a contribution to ΔN_ν , not as a source of higher T_ν . Thus, at extremely low masses, the light WIMP meets our definition of an equivalent neutrino; if the upper four curves of Fig. 1 were continued below ~ 0.1 eV, they would eventually drop to $N_{\text{eff}} = 3.02(1 + \Delta N_{\nu,\chi}/3)$, where $\Delta N_{\nu,\chi} = 4/7, 1, 8/7, \text{ or } 2$ for the particle types considered here. With the exception of the real scalar, an extremely light WIMP is a bad fit to the CMB data alone, although detailed quantitative analysis of $m_\chi \lesssim$ few eV would require dedicated modeling of CMB power spectra.

B. Primordial Abundance of ^4He

It should be noted that empirical values of the primordial helium abundance exist in the literature that differ from the value of Y_{P} we have adopted from Izotov et al. [27]. In particular, Aver et al. [54] reanalyzed a subset of the Izotov data by different methods and rejected data for individual HII regions that they considered to be poorly modeled. For the mean of the helium abundances derived from the small remaining data subset, they find 0.2535 ± 0.0036 , entirely consistent with the value $Y_{\text{P}} = 0.254 \pm 0.003$ used here. Following the usual assumption that the post-BBN helium abundance should correlate with the metallicity (*e.g.*, the oxygen abundance), Aver et al. fitted a linear regression to their helium abundance versus metallicity data and reported its intercept as Y_{P} . The small amount of data included in the Aver et al. final sample, and the small metallicity range they cover, allow a wide range of regression slopes that propagates into large errors on the inferred intercept, $Y_{\text{P}} = 0.2465 \pm 0.0097$. Within this wide range, the Aver et al. estimate overlaps with the Izotov value used here, but it provides poor parameter constraints. Given the limited data set and the limited metallicity range, in our opinion it would be a better use of these data to avoid a metallicity correction by considering the mean (perhaps restricted to the very lowest-metallicity HII regions) than to introduce an avoidable large error in the correction. Using the large Aver et al. error in our analysis allows a very wide range of ΔN_{ν} from BBN (roughly -2 to $+1.3$ at 95% confidence if there is a Majorana light WIMP, and roughly -1.5 to $+1.3$ if not), along with any value at all of m_{χ} , and it results in joint BBN+CMB constraints that are reduced nearly to those obtained from the CMB alone.

VI. SUMMARY AND CONCLUSIONS

In the absence of a light WIMP and equivalent neutrinos ($\Delta N_{\nu} \equiv 0$), BBN (in this case, SBBN) depends only on the baryon density. As shown in § III A, the SBBN-predicted abundances of deuterium and helium are a poor fit ($\chi_{\text{min}}^2 = 5.3$) to the observationally-inferred primordial abundances [25, 27], although the baryon density of this fit is in excellent agreement with the value inferred, independently, from the Planck CMB data [2]. When ΔN_{ν} is also fitted simultaneously (still without a light WIMP), an exact fit ($\chi^2 = 0$) of the two observed abundances results. Accounting for the observational uncertainties in the primordial abundances and correcting for late neutrino heating, BBN alone gives $100 \Omega_{\text{B}} h^2 = 2.29 \pm 0.06$, $\Delta N_{\nu} = 0.50 \pm 0.23$, and $N_{\text{eff}} = 3.56 \pm 0.23$ (see § III A and Fig. 4). These parameter values are in excellent agreement with those determined independently from the CMB [2], and a joint BBN + CMB fit gives $100 \Omega_{\text{B}} h^2 = 2.24 \pm 0.03$, $\Delta N_{\nu} = 0.35 \pm 0.16$ and, $N_{\text{eff}} = 3.40 \pm 0.16$ (see Fig. 5). While $\Delta N_{\nu} \leq 0$ is excluded at $\sim 98\%$ confidence (*i.e.*, 98% of the likelihood lies at $\Delta N_{\nu} > 0$), $\Delta N_{\nu} \geq 1$ is also excluded at $\gtrsim 99\%$ confidence¹⁰.

In § III C the case of an electromagnetically coupled light WIMP [1] was revisited, adopting the revised primordial D abundance [25]. The parameter estimates are changed very little from those presented in Ref. [1]. The BBN + CMB best fit remains $\Delta N_{\nu} = 0.65^{+0.45}_{-0.37}$ and (in the IND approximation, where the constant in Eqs. (7) and (8) is 3.02) $N_{\text{eff}} = 3.22 \pm 0.25$. The lower limits on m_{χ} are about 100 keV higher than those shown in Ref. [1]. Given an electromagnetically coupled light WIMP with m_{χ} in the allowed range, a sterile neutrino ($\Delta N_{\nu} = 1$) is still allowed at 1σ , while $\Delta N_{\nu} = 0$ is still disfavored.

The main focus of this paper has been the consideration of the effects on BBN (and the CMB) of a light WIMP that only couples to (and, until $T_{\gamma} \ll m_{\chi}$, remains in chemical equilibrium with) neutrinos (SM and/or equivalent; § IV and § V). We find that, well within the errors, the results for annihilation to SM neutrinos and to SM and equivalent neutrinos together are indistinguishable, and we have presented quantitative results for a WIMP that annihilates to the SM neutrinos. The key difference between this case and that of a light WIMP that annihilates to photons and/or e^{\pm} pairs is that here, as m_{χ} decreases, N_{eff}^0 increases from $N_{\text{eff}}^0 \approx 3$, instead of increasing. To maintain consistency with the Planck value of $N_{\text{eff}} \approx N_{\text{eff}}^0 + \Delta N_{\nu} = 3.30 \pm 0.27$, requires an unphysical value of $\Delta N_{\nu} < 0$ for sufficiently small WIMP masses (see Figs. 1 and 2). The increase of D and ^4He yields at low m_{χ} (Fig. 7) similarly requires $\Delta N_{\nu} < 0$ to maintain agreement with observations. Limiting ΔN_{ν} to non-negative values sets a lower bound to the WIMP mass, allowing only values in the regime where the WIMP has little effect on BBN (unless the WIMP is a real scalar, for which $m_{\chi} \ll m_e$ is not strongly ruled out). For all neutrino coupled WIMPs, the best fit WIMP mass is $m_{\chi} \geq 35$ MeV, and joint BBN + CMB fits yield $100 \Omega_{\text{B}} h^2 = 2.24 \pm 0.03$, $\Delta N_{\nu} = 0.37^{+0.16}_{-0.17}$, and (again in the IND approximation), $N_{\text{eff}} = 3.38 \pm 0.16$, in excellent agreement with the parameter values inferred without a light WIMP.

¹⁰ After the work described here was finished, we became aware of a preprint presenting a new estimate of the primordial helium abundance, $Y_{\text{P}} = 0.2551 \pm 0.0022$ [55]. This small change in the value of Y_{P} from that adopted here would, on its own, increase the BBN-inferred value of ΔN_{ν} to $\Delta N_{\nu} = 0.59 \pm 0.17$ (while reducing the error), still disfavoring both $\Delta N_{\nu} = 0$ and $\Delta N_{\nu} = 1$. Simultaneous fitting of this result with Planck parameter constraints yields $\Delta N_{\nu} = 0.45 \pm 0.13$. These new parameters, resulting from the revised Y_{P} value (and its error), are entirely consistent with the previous result within the errors of the inputs. The shift noted here would be largely canceled if the systematic difficulties with the neutron lifetime were to be resolved in favor of the beam measurements [38].

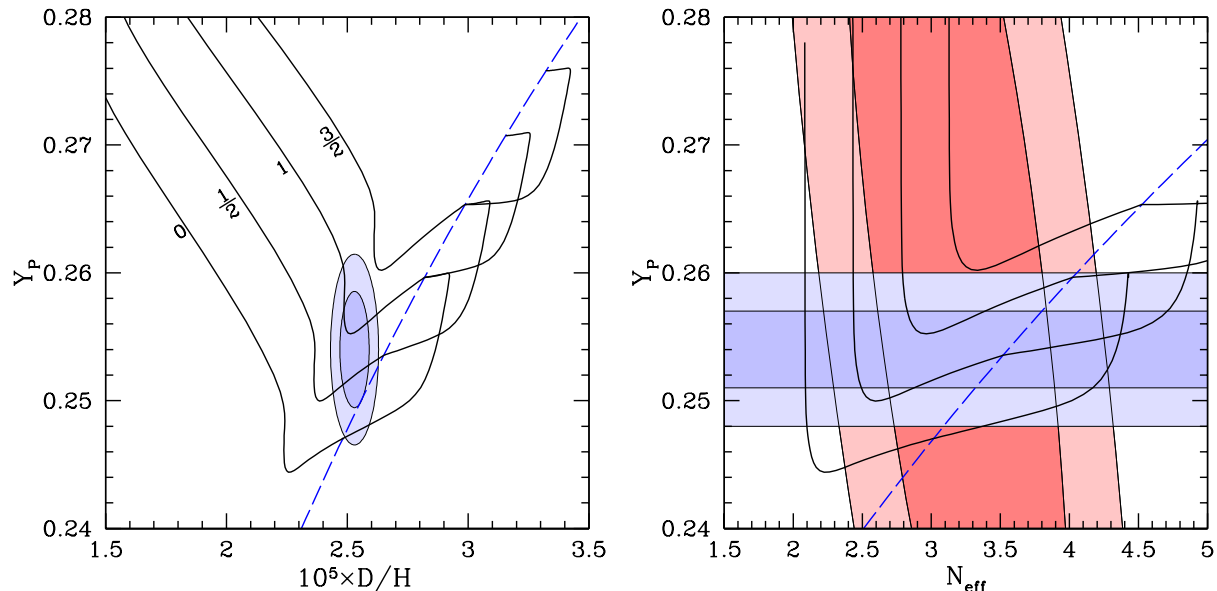


FIG. 13. (Color online) The left hand panel combines the results for Y_P versus D/H shown in Fig. 8 for the neutrino coupled WIMP, with the analogous Figure 5 of Ref. [1] for the case of an electromagnetically coupled WIMP (all at fixed $\Omega_B h^2$ from Planck). The solid (black) curves show the BBN predicted helium and deuterium abundances for several values of ΔN_ν as indicated. The dashed (blue) curve showing the $m_\chi \rightarrow \infty$ limit separates electromagnetically coupled WIMPs (on the left) from neutrino coupled WIMPs (on the right). At the upper left ends of the curves, the WIMP mass is very small. As m_χ increases, the BBN predicted abundances move along the curves, reaching the dashed curve in the high WIMP mass limit. Then, proceeding on the right side of the dashed curve, the WIMP mass decreases. The shaded contours show joint 68.3% and 95.5% contours for the observationally inferred, primordial deuterium [25] and helium [27] abundances. The right hand panel shows the analogous results for Y_P versus N_{eff} . The solid (black) curves and the solid (blue) curve correspond to those in the left hand panel. The horizontal bands (blue) are for the 68.3% and 95.5% helium abundance contours and the contours (pink) from the upper left to the lower right are from the Planck N_{eff} and Y_P fit (Ref. [2] and Table II of Ref. [1]).

As for the case of no light WIMP, for a neutrino coupled WIMP, $\Delta N_\nu = 0$ is disfavored (at $\sim 98\%$ confidence) and a sterile neutrino is excluded at $\gtrsim 99\%$ confidence.

The results presented here for neutrino coupled WIMPs and in Ref. [1] for electromagnetically coupled WIMPs may be understood in a single framework with reference to the two panels of Figure 13, which show results for Majorana WIMPs. The left hand panel, for BBN alone, shows the observationally inferred 68.3% and 95.5% confidence contours of Y_P [27] and D/H [25] adopted for the analysis here. The solid black curves show the BBN Y_P and D/H predictions at fixed (Planck Λ CDM) $\Omega_B h^2$ for WIMPs that couple electromagnetically or only to neutrinos, for four possible ΔN_ν values. At the upper left end of each curve, we have electromagnetically coupled WIMPs with very small m_χ . Descending along the curve, m_χ increases, Y_P decreases and D/H increases, eventually reaching the dashed blue curve where $m_\chi \rightarrow \infty$ (equivalent to no light WIMP). To the right of the dashed curve the WIMP is coupled to standard model neutrinos. Continuing along the solid curve, m_χ decreases, ending in the $m_\chi \rightarrow 0$ limit. For more details about this behavior, see [1] and §IV. As may be seen from the left hand panel of Fig. 13, BBN in the presence of a sufficiently light ($m_\chi \approx 5 - 10$ MeV) electromagnetically coupled WIMP favors $\Delta N_\nu > 0$ and allows a sterile neutrino ($\Delta N_\nu = 1$, but not $\Delta N_\nu = 2$). In contrast, a neutrino coupled light WIMP allows $\Delta N_\nu = 0$ but disfavors $\Delta N_\nu \gtrsim 1/2$ (at the fixed Planck Λ CDM value of $\Omega_B h^2$ shown). The agreement between BBN and the CMB reinforces these conclusions as may be seen in the $Y_P - N_{\text{eff}}$ plane in right hand panel of Fig. 13 in terms of observed Y_P and N_{eff} . Note that the CMB provides an independent, but currently very weak constraint on Y_P , allowing $N_{\text{eff}} > 4$ at 95.5% confidence. The four solid (black) curves correspond to those in the left hand panel, and the dashed (blue) curve corresponds to the dashed curve in the left hand panel. In agreement with the left panel, the combined constraints for the electromagnetically coupled case (to the left of the blue curve) slightly disfavor $\Delta N_\nu = 0$ and allow $\Delta N_\nu > 1$ (but require $\Delta N_\nu \lesssim 3/2$). For the neutrino coupled case (to the right of the blue curve), $\Delta N_\nu = 0$ is allowed and $\Delta N_\nu = 1$ is disfavored (again, at the Planck Λ CDM $\Omega_B h^2$). Thus, current BBN and CMB constraints challenge both SBBN ($\Delta N_\nu = 0$) and the presence of a sterile neutrino ($\Delta N_\nu = 1$), whether or not there is a light WIMP.

A light WIMP does not help with the primordial lithium problem. It is evident from Figs. 5 and 13 that the measured and predicted D/H agree already without a light WIMP or equivalent neutrinos. Fitting models to the

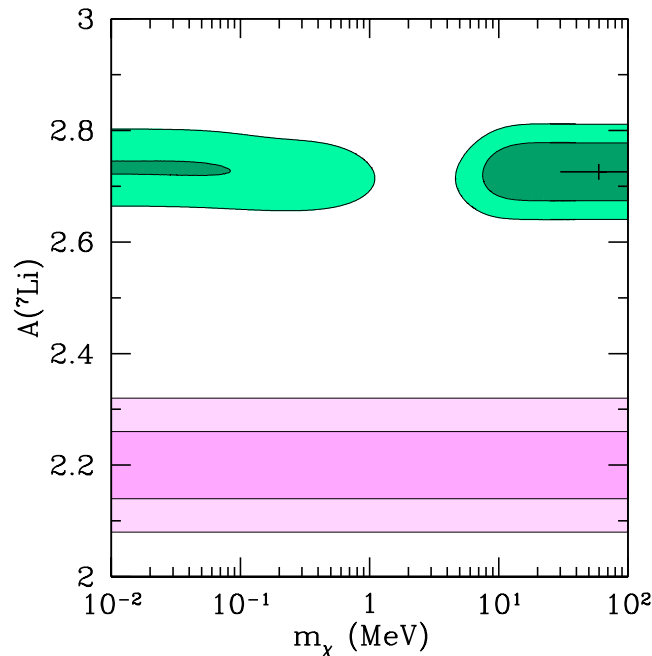


FIG. 14. (Color online) Predicted lithium abundance $A(\text{Li}) \equiv 12 + \log_{10}(\text{Li}/\text{H})$, at the 68.3% and 95.5% confidence allowed regions of our model parameters (upper curved green contours). The lower, horizontal (pink-shaded) bands show the primordial abundance inferred from halo stars in Ref. [50]. As in Fig. 11, the low- m_χ contour corresponds to the unphysical $\Delta N_\nu < 0$ regime. The thickness of the contours in the vertical direction arises mainly from nuclear uncertainties on Li production.

deuterium abundance has the effect of fixing expansion timescales late in BBN, when deuterium is burned and ${}^7\text{Li}$ (as ${}^7\text{Be}$) is created. It was found for electromagnetically coupled WIMPs in Ref. [1] that this guaranteed Li/H predictions close to the SBBN values. This remains true for the neutrino coupled WIMPs considered here. Moreover, the best fit for the neutrino coupled WIMP scenario is the high- m_χ limit: the Li/H prediction of the best-fit model is identical to that with no light WIMP, and lower WIMP masses are only allowed with compensating values of ΔN_ν , so that the Li/H prediction is the same for all m_χ . This is illustrated in Fig. 14.

In summary, the BBN and CMB data are consistent without a light WIMP. For a range of assumptions about the WIMP properties, the data imply lower limits to the allowed WIMP mass m_χ in the MeV range. An electromagnetically coupled WIMP slightly favors $m_\chi \sim 8$ MeV, but the $m_\chi \rightarrow \infty$ limit remains a quite good fit [1]. The neutrino coupled WIMPs considered here do not allow for an even slightly better fit to the data than the $m_\chi \rightarrow \infty$ limit, which is equivalent to no light WIMP at all. The analysis here excludes all neutrino coupled WIMPs with masses below a few MeV, with specific limits varying from 4 to 9 MeV depending on the nature of the WIMP. Unlike electromagnetically coupled WIMPs, there is no way to accommodate $\Delta N_\nu = 1$ by lowering the mass of a neutrino coupled WIMP; the small accommodation toward $\Delta N_\nu = 0$ allowed by a neutrino coupled WIMP is not strong enough to make $\Delta N_\nu = 0$ a good fit to the data. To avoid overinterpretation of data, it is important to consider models that provide fewer internal constraints than a “minimal” model with $\Delta N_\nu = 0$ or with only equivalent neutrinos in addition to SM particles. The particular implementations of such a nonminimal model considered here and in Ref. [1] suggest that the $\Delta N_\nu > 0$ found from abundance observations is robust to varying model assumptions.

ACKNOWLEDGMENTS

We are grateful to the Ohio State University Center for Cosmology and Astro-Particle Physics for support of G. S.’s research and for hosting K. M. N.’s visit during which most of the work described here was done. We would also like to acknowledge useful comments and suggestions from John Beacom. K. M. N. is pleased to acknowledge support from the Institute for Nuclear and Particle Physics at Ohio University, and at the University of South Carolina from U.S. Department of Energy Award No. DE-SC 0010 300 and Department of Energy Grant No. DE-FG02-09ER41621.

G. S. also acknowledges the support and hospitality of the KITP at UCSB. This research at the KITP was supported in part by the National Science Foundation under Grant No. NSF PHY11-25915.

-
- [1] K. M. Nollett and G. Steigman, *Phys. Rev. D* **89**, 083508 (2014).
 - [2] Planck Collaboration, Ade, P. A. R., et al., *A & A*, **571**, A16 (2014).
 - [3] E. W. Kolb, M. S. Turner, and T. P. Walker, *Phys. Rev. D* **34**, 2197 (1986).
 - [4] P. D. Serpico and G. G. Raffelt, *Phys. Rev. D* **70**, 043526 (2004).
 - [5] C. Boehm, T. A. Ensslin, and J. Silk, *J. Phys. G* **30**, 279 (2004).
 - [6] C. Boehm and P. Fayet, *Nucl. Phys. B* **683**, 219 (2004).
 - [7] C. Boehm, D. Hooper, J. Silk, M. Casse, and J. Paul, *Phys. Rev. Lett.* **92**, 101301 (2004).
 - [8] D. Hooper, F. Ferrer, C. Boehm, J. Silk, J. Paul, N. W. Evans, and M. Casse, *Phys. Rev. Lett.* **93**, 161302 (2004).
 - [9] C. Boehm, P. Fayet, and J. Silk, *Phys. Rev. D* **69**, 101302 (2004).
 - [10] K. Ahn and E. Komatsu, *Phys. Rev. D* **72**, 061301 (2005).
 - [11] P. Fayet, D. Hooper, and G. Sigl, *Phys. Rev. Lett.* **96**, 211302 (2006).
 - [12] D. Hooper, M. Kaplinghat, L. E. Strigari, and K. M. Zurek, *Phys. Rev. D* **76**, 103515 (2007).
 - [13] D. Hooper and K. M. Zurek, *Phys. Rev. D* **77**, 087302 (2008).
 - [14] J. L. Feng and J. Kumar, *Phys. Rev. Lett.* **101**, 231301 (2008).
 - [15] G. Steigman, *Phys. Rev. D* **87**, 103517 (2013).
 - [16] C. M. Ho and R. J. Scherrer, *Phys. Rev. D* **87**, 023505 (2013).
 - [17] C. M. Ho and R. J. Scherrer, *Phys. Rev. D* **87**, 065016 (2013).
 - [18] C. Boehm, M. J. Dolan, and C. McCabe, *JCAP* **12** (2012) 027.
 - [19] G. Mangano, G. Miele, S. Pastor, T. Pinto, O. Pisanti, and P. D. Serpico, *Nucl. Phys. B* **729**, 221 (2005).
 - [20] S. Dodelson and L. M. Widrow, *Phys. Rev. Lett.* **72**, 17 (1994).
 - [21] C. Boehm, M. J. Dolan, and C. McCabe, *JCAP* **08** (2013) 041.
 - [22] A. D. Dolgov, S. L. Dubovsky, G. I. Rubtsov, and I. I. Tkachev, *Phys. Rev. D* **88**, 117701 (2013).
 - [23] K. C. Y. Ng and J. F. Beacom, *Phys. Rev. D* **90**, 065035 (2014).
 - [24] B. Ahlgren, T. Ohlsson, and S. Zhou, *Phys. Rev. Lett.* **111**, 199001 (2013).
 - [25] R. J. Cooke, M. Pettini, R. A. Jorgenson, M. T. Murphy, and C. C. Steidel, *Astrophys. J.* **781**, 31 (2014).
 - [26] G. Steigman, *J. Cosmol. Astropart. Phys.* **10** (2006) 016.
 - [27] Y. I. Izotov, G. Stasinska, and N. G. Guseva, *A & A* **558**, A57 (2013).
 - [28] K. Enqvist, K. Kainulainen, and V. Semikoz, *Nucl. Phys. B* **374**, 392 (1992).
 - [29] A. D. Dolgov, *Phys. Rept.* **370**, 333 (2002).
 - [30] S. Hannestad, *Phys. Rev. D* **65**, 083006 (2002).
 - [31] J. Chluba, *MNRAS* **443**, 1881 (2014).
 - [32] D. J. Fixsen, E. S. Cheng, J. M. Gales, J. C. Mather, R. A. Shafer, and E. L. Wright, *Astrophys. J.* **473**, 576 (1996).
 - [33] J. L. Feng, H. Tu, and H.-B. Yu, *JCAP* **10** (2008) 043.
 - [34] L. Kawano, Fermilab-PUB-88/34-A (1998).
 - [35] L. Kawano, Fermilab-PUB-92/04-A (1992).
 - [36] J. Beringer *et al.* (Particle Data Group), *Phys. Rev. D* **86**, 010001 (2012).
 - [37] K. A. Olive *et al.* (Particle Data Group), *Chin. Phys. C*, **38**, 090001 (2014).
 - [38] F. E. Wietfeldt and G. L. Greene, *Rev. Mod. Phys.* **83**, 1173 (2011).
 - [39] L. Ma, H. J. Karwowski, C. R. Brune, Z. Ayer, T. C. Black, J. C. Blackmon, E. J. Ludwig, M. Viviani, A. Kievsky, and R. Schiavilla, *Phys. Rev. C* **55**, 588 (1997).
 - [40] E. G. Adelberger *et al.*, *Rev. Mod. Phys.* **83**, 195 (2011).
 - [41] M. Viviani, A. Kievsky, L. E. Marcucci, S. Rosati, and R. Schiavilla, *Phys. Rev. C* **61**, 064001 (2000).
 - [42] L. E. Marcucci, M. Viviani, R. Schiavilla, A. Kievsky, and S. Rosati, *Phys. Rev. C* **72**, 014001 (2005).
 - [43] K. M. Nollett and G. P. Holder (2011), arXiv:1112:2683 [astro-ph.CO].
 - [44] E. Di Valentino, C. Gustavino, J. Lesgourgues, G. Mangano, A. Melchiorri, G. Miele, and O. Pisanti, *Phys. Rev. D* **90**, 023543 (2014).
 - [45] L. Salvati, N. Said, and A. Melchiorri, *Phys. Rev. D* **90**, 103514 (2014).
 - [46] G. Steigman, *Ann. Rev. Nucl. Part. Sci.* **57**, 463 (2007).
 - [47] M. Pettini and R. Cooke, *MNRAS* **425**, 2477 (2012).
 - [48] W. A. Rolke, A. M. López, and J. Conrad, *Nucl. Inst. & Methods A* **551**, 493 (2005).
 - [49] B. D. Fields, *Ann. Rev. Nucl. Part. Sci.* **61**, 47 (2011).
 - [50] M. Spite, F. Spite, and P. Bonifacio, *Mem. Soc. Astron. Ital.* **22**, 9 (2012).
 - [51] J. F. Beacom, N. F. Bell, and G. D. Mack, *Phys. Rev. Lett.* **99** 231301 (2007).
 - [52] S. Palomares-Ruiz and S. Pascoli, *Phys. Rev. D* **77** 025025 (2008).
 - [53] W.-C. Huang and F. F. Deppisch, (2014) arXiv:1412.2027 [hep-ph]
 - [54] E. Aver, K. A. Olive, R. L. Porter, and E. D. Skillman, *JCAP* **11** (2013)017.
 - [55] Y. I. Izotov, T. X. Thuan, and N. G. Guseva, (2014) arXiv:1408.6953 [astro-ph.CO]